

1 **Assessing Exposure to Climate Extremes over the Arabian**
2 **Peninsula Using ERA5 Reanalysis Data: Spatial Distribution and**
3 **Temporal Trends**

4
5 Ali Salem Al-Sakkaf ^{1,2}, Zhang Jiahua ³, Yao Fengmei ^{1,*}, Mohammed Magdy
6 Hamed ^{4,5}, Claudien Habimana Simbi ¹, Arslan Ahmed ¹, and Shamsuddin Shahid ⁵

7
8 ¹ College of Earth and Planetary Sciences, University of Chinese Academy of Sciences
9 (UCAS), Beijing 100049, China.

10 ² Yemen Meteorological Services, Civil Aviation & Meteorology Authority (CAMA),
11 Sana'a 7145, Yemen.

12 ³ Centre for Remote Sensing & Digital Earth, College of Computer Science &
13 Technology, Qingdao University, Qingdao, China

14 ⁴ Construction and Building Engineering Department, College of Engineering and
15 Technology, Arab Academy for Science, Technology and Maritime Transport
16 (AASTMT), B 2401 Smart Village, 12577, Giza, Egypt

17 ⁵ Department of Water and Environmental Engineering, Faculty of Civil Engineering,
18 Universiti Teknologi Malaysia (UTM), 81310 Skudua, Johor, Malaysia

19
20 *Corresponding Author E-mail: yaofm@ucas.ac.cn (Y. F)

26 **Assessing Exposure to Climate Extremes over the Arabian Peninsula Using** 27 **ERA5 Reanalysis Data: Spatial Distribution and Temporal Trends**

28 **Abstract**

29 Understanding climate extremes and indices is crucial for addressing climate change impacts,
30 including the increased variability in local weather patterns and extreme events. Previous
31 studies on the Arabian Peninsula (AP) have been limited by sparse station data and restricted
32 spatial coverage. To overcome this limitation, this paper aims to assess the spatial distribution
33 and temporal trends of temperature and precipitation indices suggested by the Expert Team on
34 Climate Change Detection and Indices (ETCCDI) using ERA5 reanalysis data from 1951 to
35 2020 for the AP. Additionally, this study investigated the changes relative to the reference
36 period (1951–1980). The modified Mann-Kendall test and Sen's Slope estimator are utilized to
37 detect significant trends and estimate their magnitude. Results revealed that ERA5 was
38 consistent with previous studies that utilized in-situ station data, offering a more detailed
39 picture of the affected areas. The findings indicated a significant warming trend in temperature
40 indices, with an increase of over 1°C per decade observed across several areas, including the
41 northern AP, and certain regions experiencing a discrepant change of 3°C increase compared
42 to the reference period. Changes in rainfall indices indicate a shift in rainfall patterns from the
43 AP's fertile southwest regions towards more intense patterns in specific eastern regions,
44 including Oman, Kuwait, Saudi Arabia, and Yemen. However, the precipitation temporal
45 trends are weak in magnitude and variable spatially, with dominant decreases in both intensity
46 (-10 mm per decade) and frequency indices (-5 days per decade). Some locations are subject
47 to the combined effects of most heatwave indicators simultaneously, while flood indicators and
48 yet others by drought indicators influence others. All these locations have been accurately
49 identified in this study. The findings provide valuable information regarding the region's
50 climate change vulnerability and adaptation needs.

51 **Keywords:** Arabian Peninsula; ERA5; Climate indices; Significant trends; Yemen

52 1. Introduction

53 Climate change is now among the most urgent challenges of the century (WHO, 2018), with
54 significant effects on human life, ecosystems, and economic activities. Among the various
55 aspects of the changing climate, the study of climate extremes is of particular importance, as
56 they are often associated with high-impact events such as heatwaves, droughts, and heavy
57 precipitation that can cause severe damage to both natural systems and human lifestyle
58 (Easterling et al., 2000; Fischer et al., 2021). In this context, the Expert Team on Climate
59 Change Detection and Indices (ETCCDI) has suggested a broad set of indicators to examine
60 extremes in the climate (Karl et al., 1999), which have been extensively employed in various
61 regional and global analyses. Research on climate extremes and indices and their trends is an
62 important topic among researchers to measure and verify climate change in an area of interest.
63 To that end, numerous investigations have been conducted on both a regional and national scale
64 in diverse regions worldwide (Ahmed et al., 2017; Bhatti et al., 2020; Donat et al., 2014;
65 Gunawardhana et al., 2018; Islam et al., 2021; Nashwan et al., 2019; Ng et al., 2022; Shahid,
66 2010; Walt and Fitchett, 2021; Zhang et al., 2005; Zittis et al., 2022). Understanding previous
67 TempPrec extremes is critical for designing more extensive and long-term climate resilience
68 measures (Hamed 2021; Yu et al. 2015). Assessing variations in rainfall extremes is critical in
69 order to estimate the potential implications of climate change, such as catastrophic floods and
70 prolonged periods of drought, as well as organizing climate change mitigation and adaption
71 strategies (Almazroui and Saeed, 2020; Kotwicki and al Sulaimani, 2009). The severe
72 implications of TempPrec extremes mean that extensive study on them utilizing longer records
73 is necessary for each country or region (Odnoletkova and Patzek, 2021). This is especially
74 significant for the AP, which has a semiarid and arid environment (Almazroui, 2020a;
75 Kwarteng et al., 2009).

76 The Arabian Peninsula (AP) region is vulnerable to climate variability and change,
77 especially climate extremes, which can significantly impact water resources, agriculture, and
78 human health (Almazroui et al., 2022; Donat et al., 2014; Zhang et al., 2005). Consequently,
79 several studies of climatic extremes over AP have been undertaken (Almazroui et al., 2022;
80 Alsarmi and Washington, 2014; Donat et al., 2014; Zhang et al., 2005). Almazroui et al. (2022)
81 examined temperature and precipitation (TempPrec) extremes over Saudi Arabia during 1978-
82 2021. It revealed significant trends in climate extremes, including increased heatwaves and
83 heavy precipitation events. Alsarmi and Washington (2014) used in-situ observations from 23
84 stations spread over the AP from 1970 to 2008. They found significant warming trends, while
85 precipitation trends were slight and insignificant, except for the PRCPTOT (annual total

86 precipitation in wet days) index. Donat et al. (2014) collected in-situ observations from 61
87 stations across the Middle East and North Africa (MENA), including 13 stations in the AP,
88 from 1961 to 2010. Their findings indicated warming trends throughout the region, with
89 precipitation patterns exhibiting reduced uniformity, increased temporal and spatial variability,
90 and a prevalence of drying trends in the AP. Zhang et al. (2005) analyzed in-situ observations
91 from 52 stations in the Middle East, including 9 stations only in the AP, from 1950 to 2003,
92 revealing a considerable rise in temperature extremes such as warm days and nights, as well as
93 changes in precipitation patterns, including an increase in consecutive dry days. Excluding data
94 from in-situ meteorological stations, Khan et al. (2019) utilized the daily gridded precipitation
95 dataset APHRODITE (Asian Precipitation Highly Resolved Observational Data Integration
96 Towards Evaluation) over Malaysia and showed a drop in rainy days together with a rise in
97 wet spells and the maximum one-day precipitation. ERA5 reanalysis data was utilized by
98 Odnoletkova and Patzek (2021) to investigate trends in temperature extremes and human
99 comfort indices in Saudi Arabia from 1979 to 2019, revealing significant warming trends in all
100 seasons, along with an increase in the frequency and intensity of heatwaves, which have
101 negative impacts on human comfort and health. Most previous studies have utilized the Mann-
102 Kendall (MK) test (Hamed, 2008) and Sen's slope estimator (Sen, 1968). However, there is a
103 lack of studies that have employed the Modified Mann-Kendall (MMK) test on the AP, which
104 is considered superior (Khan et al., 2019). Khan et al. (2019) employed the MK and MMK
105 tests, revealing that the MMK test rejected most of the significant trends observed by the MK
106 test over Malaysia and provided more details.

107 Most studies conducted earlier have examined TempPrec extremes over the AP.
108 However, it is worth noting that most of these studies, regardless of their quality, relied on
109 sparse station records and limited temporal periods. As a consequence, there are fewer spatial
110 coverages, particularly over remote areas such as deserts and mountains (Almazroui et al.,
111 2022, 2014; AlSarmi and Washington, 2014; Gunawardhana et al., 2018; Hereher, 2016; Zhang
112 et al., 2005). Across AP, Donat et al. (2014) used data from 13 stations, Zhang et al. (2005)
113 used nine stations, and AlSarmi and Washington (2011, 2014) used 21 and 23 stations,
114 respectively. Tarawneh and Chowdhury (2018) used data from only three stations in Saudi
115 Arabia. Recently, Almazroui et al. (2022) used data from 24 stations in Saudi Arabia, which
116 covers around 80% of the AP's area. However, many places in the AP lack sufficient stations,
117 such as Yemen, which ranked the peninsula's second-largest nation, covering 527,970 km²
118 (AL-wesabi et al., 2022). Moreover, the terrain in the AP is diverse, with towering mountains,
119 plateaus, plains, valleys, and coasts, all of which necessitate more densely well-distributed

120 monitoring stations to observe meteorological phenomena in these areas as per the
121 requirements laid out by the World Meteorological Organization (WMO) within its "Guide to
122 Meteorological Instruments and Methods of Observation WMO-No. 8" (WMO, 2021) for
123 station density thresholds and guidelines that are challenging to fully conform to Giazzi et al.
124 (2022). To fill these gaps, this study employs the ERA5 reanalysis dataset, a cutting-edge
125 worldwide climate reanalysis product prepared by the European Centre for Medium-Range
126 Weather Forecasts (ECMWF). Using ERA5 data offers an unprecedented opportunity to
127 overcome the data scarcity issue in the AP, as it provides a consistent and high-resolution
128 representation of climate variables across the entire region, including areas with limited or no
129 observational stations.

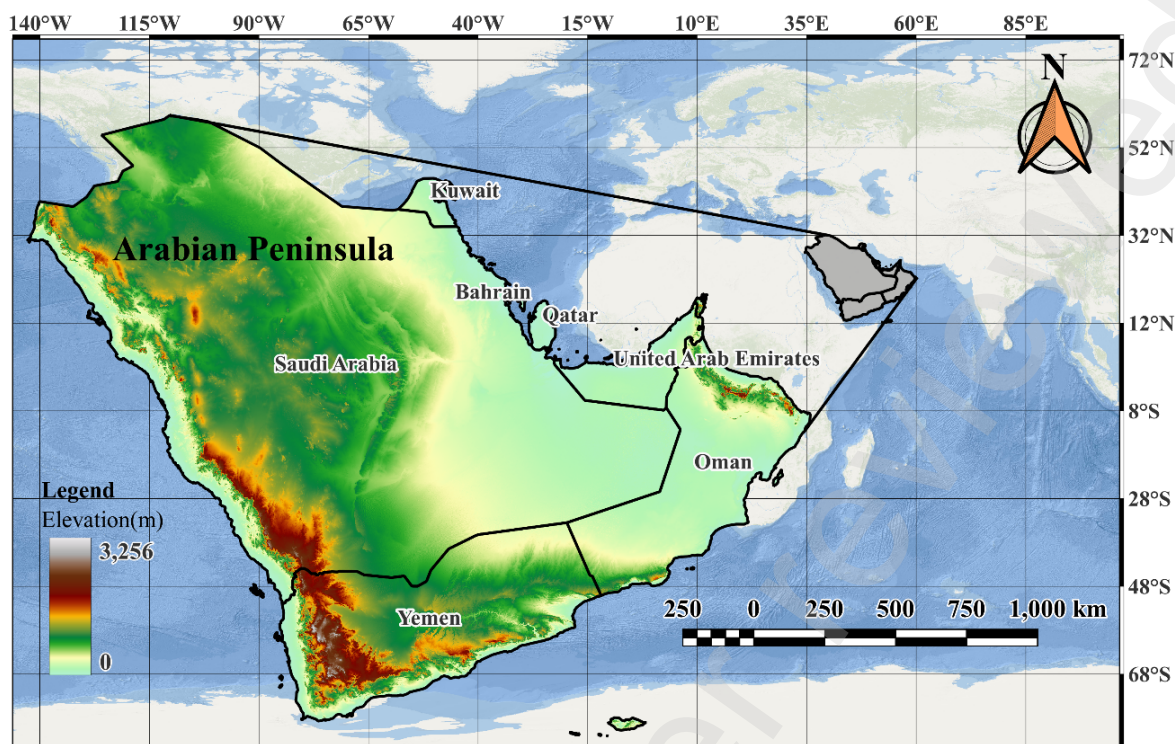
130 This research utilizes the ERA5 reanalysis data to investigate both temperature and
131 precipitation extremes and trends using MMK over the whole AP, which will contribute
132 significantly to advancing our understanding of this topic in this region. Under the stress of
133 climate change and population inflow to this region, this research aims to characterize the
134 geographical distribution of trends and changes in TempPrec indices within AP from 1951 to
135 2020, based on the indices suggested by ETCCDI using ERA5 reanalysis data. Specifically,
136 the study aims to (1) identify the spatial changes in TempPrec indices over AP, (2) examine
137 the temporal trends of these indices over the study period, and (3) highlight climate-affected
138 areas, including those prone to heatwaves, droughts, and floods, for long-term socioeconomic
139 planning. The findings of this investigation will shed light on the changing nature of climate
140 extremes in the AP, which could inform decision-making processes related to the region's
141 climate change adaptation and risk management. The study's findings will likely provide the
142 groundwork for future studies on the region's impact of global warming.

143

144 **2. Study Area and Data**

145 **2.1. Arabian Peninsula**

146 The Arabian Peninsula (latitude 12–33°N and longitude 34–61°E) is a historical, vast, and
147 diverse region in the Middle East, covering a significant portion of the Arabian subcontinent
148 (**Fig. 1**). The peninsula covers an area of approximately 3.2 million km². It includes the
149 following countries listed from largest to smallest in terms of area: Saudi Arabia, Yemen,
150 Oman, the United Arab Emirates (UAE), Kuwait, Qatar, and Bahrain. The AP has a diverse
151 landscape, varying from the coastline along the Arabian Gulf and the Red Sea to deserts and
152 mountains in the interior with elevations of more than 3,000 m.



154

Fig. 1. The study area location with elevation.

155

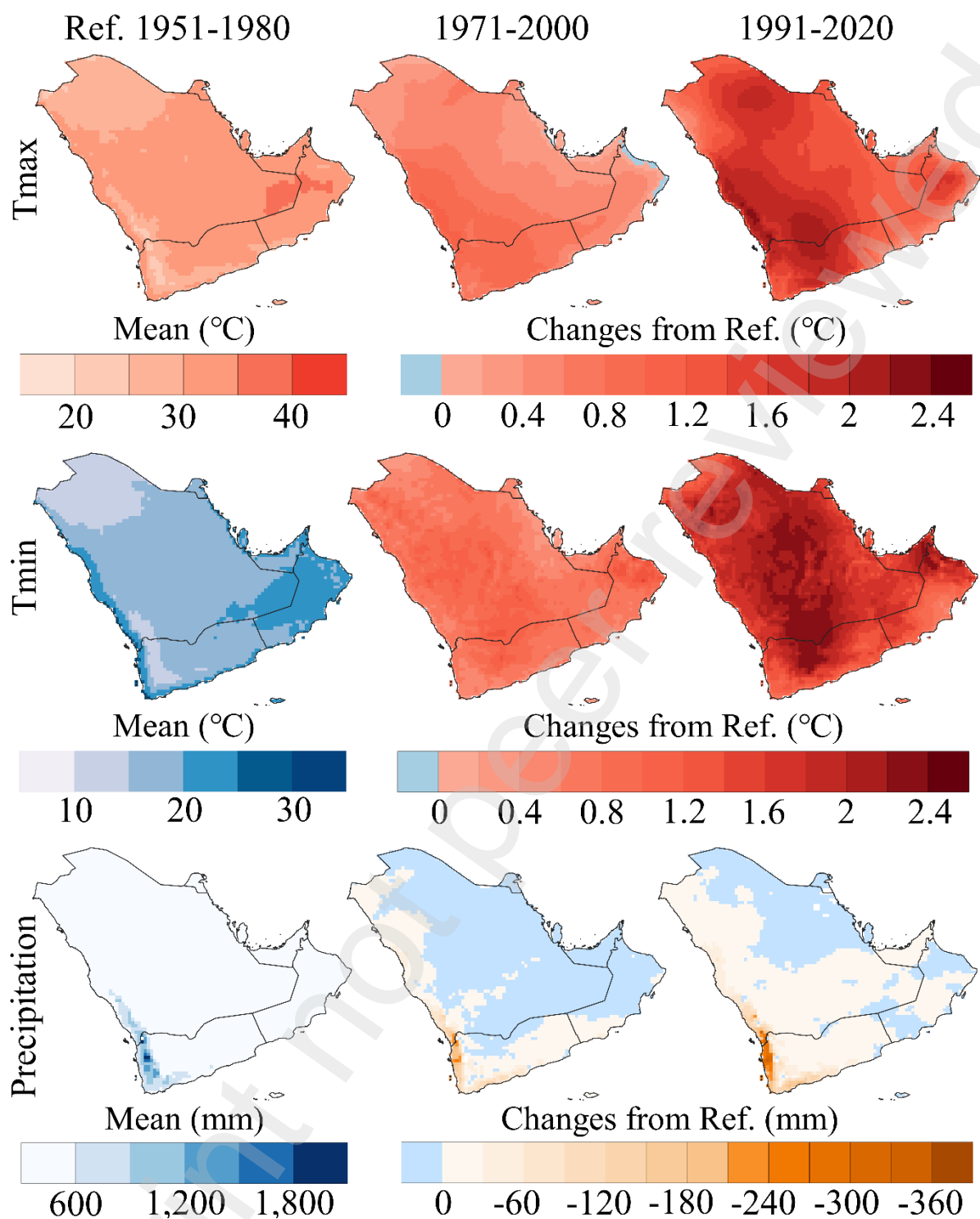
156

157 AP is characterized by a predominantly arid climate with vast deserts and rugged
 158 mountains. Despite its harsh environmental conditions, the region has considerable social and
 159 economic significance, being home to millions of people and playing a crucial role in global
 160 energy production and trade (Sedaoui, 2022). The AP represents the most significant global
 161 reservoir of petroleum (Saleh M. Billo, 1982). The augmentation of the economy in nations
 162 including Qatar, the UAE, Bahrain, Saudi Arabia, Kuwait, and Oman has attracted a large
 163 influx of migrant workers to the AP, making them hubs for business and commerce due to
 164 abundant petroleum resources (Aker and Aghaei, 2019). However, the AP's harsh climate,
 165 water scarcity, and reliance on fossil fuels make it particularly susceptible to the influences of
 166 climate change (Almazroui et al., 2017). **Fig. 2** depicts the magnitude of the AP's vulnerability
 167 to climate change. It reflects the rapid tendency and impact of change over the past seven
 168 decades in the AP. The left column in **Fig. 2** shows the daily mean values for the reference
 169 period (1951-1980). The middle and right columns depict the changes from the reference
 170 period during the second period (1971-2000), and the recent period (1991-2020), respectively.
 171 The temperature changes clearly reflect how much the AP has been influenced by global
 172 warming. Certain regions currently experience a warming of more than 2°C difference
 173 compared to the reference period. The amounts of rainfall received in the AP have decreased

174 dramatically compared to the reference period, requiring urgent action and full preparedness
175 for the resulting consequences.

176 Given the accelerated urbanization and population influx in this region, understanding the
177 influence of climate extremes is crucial for developing sustainable development policies and
178 strategies (Lin et al., 2020; Zhao et al., 2019). Diverse climatic conditions, including arid
179 deserts, coastal areas, and high-altitude mountains, distinguish the AP. The AP climate is
180 dominated by the Indian monsoon's effect and the movements of the Inter-Tropical
181 Convergence Zone (Almazroui et al., 2012). Climatic extremes, such as high temperatures,
182 heavy rainfall, and drought, are common over the AP and can have significant environmental,
183 social, and economic impacts (AlSarmi and Washington, 2011).

184



185

186 **Fig. 2.** Spatial distribution of the changes in the key climate variables used in this study:
 187 maximum temperature (Tmax), minimum temperature (Tmin), and precipitation.

188

189 2.2. ERA5

190 The insufficiency of observation stations goes against the rising requirements of the scientific
191 community (You et al., 2013), particularly when it comes to evaluating extreme events (Donat
192 et al., 2014). As a result, climate change analysis requires long-term data and a fine spatial
193 resolution (Lei et al., 2022). Studies on climate extremes and their trends are predominantly
194 reliant on rainfall and Tmin/Tmax that is observed via in-situ meteorological stations
195 (Almazroui et al., 2022; Alsarmi and Washington, 2014; Donat et al., 2014; Gunawardhana et
196 al., 2018; Islam et al., 2021; Ng et al., 2022; Zhang et al., 2005). Although utilizing
197 meteorological stations in the AP yields some positive results, several drawbacks still exist
198 (Donat et al., 2014). This is attributed to the inequitable distribution of the in-situ observations
199 across AP and the inadequate count of stations, as well as missing data, which usually results
200 in unsatisfactory spatiotemporal features, especially in the vast regions of the Rub Al-Khali
201 desert (or Empty Quarter) and Yemen, where the meteorological stations are very sparse. To
202 overcome this, other datasets have been used. These datasets can be split into three categories
203 depending on the data sources and models used: satellite-based datasets, interpolated surface
204 observation datasets, and reanalysis datasets (Jiang et al., 2021).

205 This study used reanalysis data because it is an excellent choice when it comes to
206 climatological applications due to its fine spatiotemporal resolution, diverse data
207 classifications, and worldwide extent (Kaiser-Weiss et al., 2019; Kalnay et al., 1996;
208 Mavromatis, 2022). The reanalysis datasets have been extensively used as compared to the
209 other two data categories (Fonseca et al., 2022; Golshani et al., 2022; Lei et al., 2022).
210 Advancements in data assimilation techniques, satellite remote sensing, land surface, and
211 atmospheric models have gradually increased the temporal and spatial resolution of reanalysis
212 datasets (Nakamura et al., 2022). ERA5 reanalysis data was chosen over other reanalysis
213 datasets because it has a higher spatial resolution (0.25° , ~ 31 km), temporal resolution (hourly),
214 and temporal coverage (1940-present). It also performs better over the AP than other frequently
215 utilized reanalysis datasets (Fonseca et al., 2022; Odnoletkova and Patzek, 2021). The ERA5
216 reanalysis dataset was created by utilizing a vast array of measurement and remote sensing data
217 through a retrospective analysis of historical information by the European Center for Medium-
218 Range Weather Forecasts (Hersbach et al., 2020). ERA5 is the fifth-generation reanalysis
219 dataset, an extension of the well-known ERA product family, including ERA-Interim and
220 ERA-40, created by the ECMWF.

221 Several studies used ERA5 to investigate climate extremes (Ali et al., 2023; Lei et al.,
222 2022; Li et al., 2022; Xu et al., 2022; Zhao et al., 2023). Li et al. (2022) utilized the ERA5
223 reanalysis dataset to examine the period and quantity of frost days in response to climate
224 change. Avila-Diaz et al. (2021) investigated TempPrec extremes as defined by the ETCCDI
225 for regional and global reanalysis datasets. Their study revealed that ASRv2 and ERA5 show
226 the highest levels of performance. ERA5 has been used for many research studies over AP (Al-
227 Mutairi et al., 2023; Fonseca et al., 2022; Francis et al., 2021; Golshani et al., 2022; Saeed et
228 al., 2023; Safieddine et al., 2022). Fonseca et al. (2022) examined the climate conditions and
229 seasonal changes in the AP from 1979 to 2019 using ERA5 data. Saeed et al. (2023) studied
230 how circulation patterns in mid-latitudes affect the variability of winter temperatures in the AP
231 by utilizing NCEP and ERA5 reanalysis data. The ERA5 data were validated against
232 observations from weather stations worldwide (Li et al., 2020) and over major towns in Saudi
233 Arabia and showed good performance (Odnoletkova and Patzek, 2021). However, AL-Falahi
234 et al. (2020) reported that the efficacy of ERA5 in predicting rainfall rates in Yemen's highland
235 region was limited due to the location's characteristics and the limited ground stations. It may
236 also result from insufficient quality control procedures for the station data before use.
237 Nevertheless, numerous investigations have assessed the ERA5 dataset across the globe and
238 found better-performing results (Alriah et al., 2022; Arshad et al., 2021; Dubache et al., 2021;
239 Hamed et al., 2021; Ma et al., 2021; Randriatsara et al., 2022). Arshad et al. (2021) revealed
240 that ERA5 accurately tracks rain gauges across various climate regions in Pakistan.
241 Furthermore, the ERA5 dataset has been extensively employed as a point of reference in many
242 studies conducted across the AP (Bawadekji et al., 2022; Francis et al., 2021; Horan et al.,
243 2023; Komurcu et al., 2020; Odnoletkova and Patzek, 2021; Safieddine et al., 2022) and other
244 regions (Ali et al., 2023; Hamed et al., 2023b, 2022; Khadka et al., 2022; Zuluaga et al., 2021).

245 For this study, hourly precipitation and 2m temperature records from 1951 to 2020 were
246 employed to determine rainfall, Tmax, and Tmin daily data. This data was sourced from the
247 latest reanalysis, ERA5, developed by ECMWF (Hersbach et al., 2020). Regardless of the
248 climate in AP, this study used ERA5 to analyze all ETCDDI indices. The ETCDDI details can
249 be found in

250

251

252 **Table 1.**

253

254

255 **Table 1**

256 Definitions of the ETCCDI indices that were utilized in this study.

El. IDs	Indicator Name	Definition	Units
<i>Duration indices</i>			
FD	Frost days	Annual count of days when daily Tmin < 0° C.	
ID	Icing days	Annual count of days when daily Tmax < 0° C.	
SU	Summer days	Annual count of days when daily Tmax > 25° C.	
TR	Tropical nights	Annual count of days when daily Tmin > 20° C.	
WSDI	Warm spell duration indicator	Annual count of days with at least 6 consecutive days when Tmax>90th percentile.	Days
CSDI	Cold spell duration indicator	Annual count of days with at least 6 consecutive days when Tmin>10th percentile.	
GSL	Growing season length	Annual (1st Jan to 31st Dec in Northern Hemisphere (NH)) count between the first span of at least 6 days with daily mean temperature >5°C.	
<i>Absolute indices</i>			
TXx	Max Tmax	Annual mean of monthly max value of daily Tmax	
TNx	Max Tmin	Annual mean of monthly max value of daily Tmin	
TXn	Min Tmax	Annual mean of monthly min value of daily Tmax	°C
TNn	Min Tmin	Annual mean of monthly min value of daily Tmin	
DTR	Diurnal temp. range	Annual mean difference between Tmax and Tmin	
<i>Relative indices</i>			
TN10p	Cool nights	Percentage of days when Tmin < 10th percentile	
TN90p	Warm nights	Percentage of days when Tmin > 90th percentile	%
TX10p	Cool days	Percentage of days when Tmax < 10th percentile	
TX90p	Warm days	Percentage of days when Tmax > 90th percentile	
<i>Intensity indices</i>			
RX1day	Max 1 day PR amount	Annual max 1-day precipitation (PR)	
RX5day	Max 5 days PR amount	Annual max consecutive 5-day PR	
SDII	Simple daily intensity index	Annual total PR divided by the number of wet days (defined as PR >=1.0mm) in the year	mm
R95pTOT	Very wet days	Annual total PR when PR >95th percentile	
R99pTOT	Extremely wet days	Annual total PR when PR >99th percentile	
PRCPTOT	Annual total wet-day PR	Annual total PR in wet days (PR >=1mm)	
<i>Frequency indices</i>			
R10	Heavy PR days	Annual count of days when PR >=10mm	
R20	Very heavy PR days	Annual count of days when PR >=20mm	
CDD	Consecutive dry days	Max number of consecutive days with PR <1mm	Days
CWD	Consecutive wet days	Max number of consecutive days with PR >=1mm	

257 More details on definitions of the core indices given at
 258 http://etccdi.pacificclimate.org/list_27_indices.shtml

259 3. Methodology

260 The Expert Team on Climate Change Detection and Indices (ETCCDI) was established by
261 Frich et al. (2002) to present a wide range of climate indices and indicators with the goal of
262 creating relevant extreme indices that are consistent across wide territories. The ETCCDI
263 suggests a comprehensive compilation of 27 fundamental indices, comprising 11 indices for
264 rainfall and 16 indices for temperature.

265

266

267 Table 1 summarizes the ETCCDI indices utilized in this study. The ETCCDI indices allow for
268 direct monitoring of climate trend strength and frequency. Therefore, these indices were used
269 in this study due to the comprehensive list of the indices being provided and its suitability to
270 be employed for comparative assessment (Sa'adi et al., 2023). The analysis was performed
271 using R (v4.1.3; R Core Team 2023) code script. All ETCCDI core indices of extreme climate
272 were calculated by the *climdex.pcic* R package (David Bronaugh, 2020). This package contains
273 functions such as *climdex.su* and *climdex.id* to compute all climate indices at each grid box
274 based on the input data and assign the result to a corresponding variable. There are 3927 grid
275 boxes throughout the AP. The code then processed time series data, calculated extreme values,
276 and generated raster files for different measures and time periods. Furthermore, Sen's Slope
277 and MMK tests were calculated using the functions *sens.slope* and *pwmk* from the packages
278 *trend* (Pohlert, 2023) and *modifiedmk* (Patakamuri and O'Brien, 2021), respectively. Finally, the
279 spatiotemporal maps of the climate indices and their trends throughout all periods were
280 prepared using QGIS software (QGIS Development Team, 2023).

281 A 30-year time frame with overlapping 10-year periods was utilized to examine the
282 changing patterns of the extremes. The 30 years (1951-1980) was selected as a reference
283 period, and the other two periods (1971-2000 and 1991-2020) to represent the change or
284 difference from the reference period (Hamed et al., 2023b). In this study, the MMK test was
285 used to determine the significance of the trend in the variables explored, while Sen's Slope was
286 used to quantify the change. Sen's Slope and MK have both been extensively utilized in the
287 literature. The MMK test is deemed to be more precise and adaptable than the original MK test
288 in detecting patterns in hydro-meteorological records (Khan et al., 2019; Nashwan et al., 2019).
289 MMK is less likely to falsely detect a trend in autocorrelated data, such as the data used in this

290 study (Yue and Wang, 2004). The slopes (T) between any two successive points of data in a
291 time series of (N) observations are used to calculate the rate of change (Q_s):

$$Q_s = \begin{cases} \frac{T(N+1)}{2} & \text{if } N \text{ is odd} \\ \frac{\frac{TN}{2} + T\left(\frac{N+2}{2}\right)}{2} & \text{if } N \text{ is even} \end{cases} \quad (1)$$

292 A positive Q_s number represents an increase, whereas a negative value represents a
293 decrease.

294

295 **4. Results**

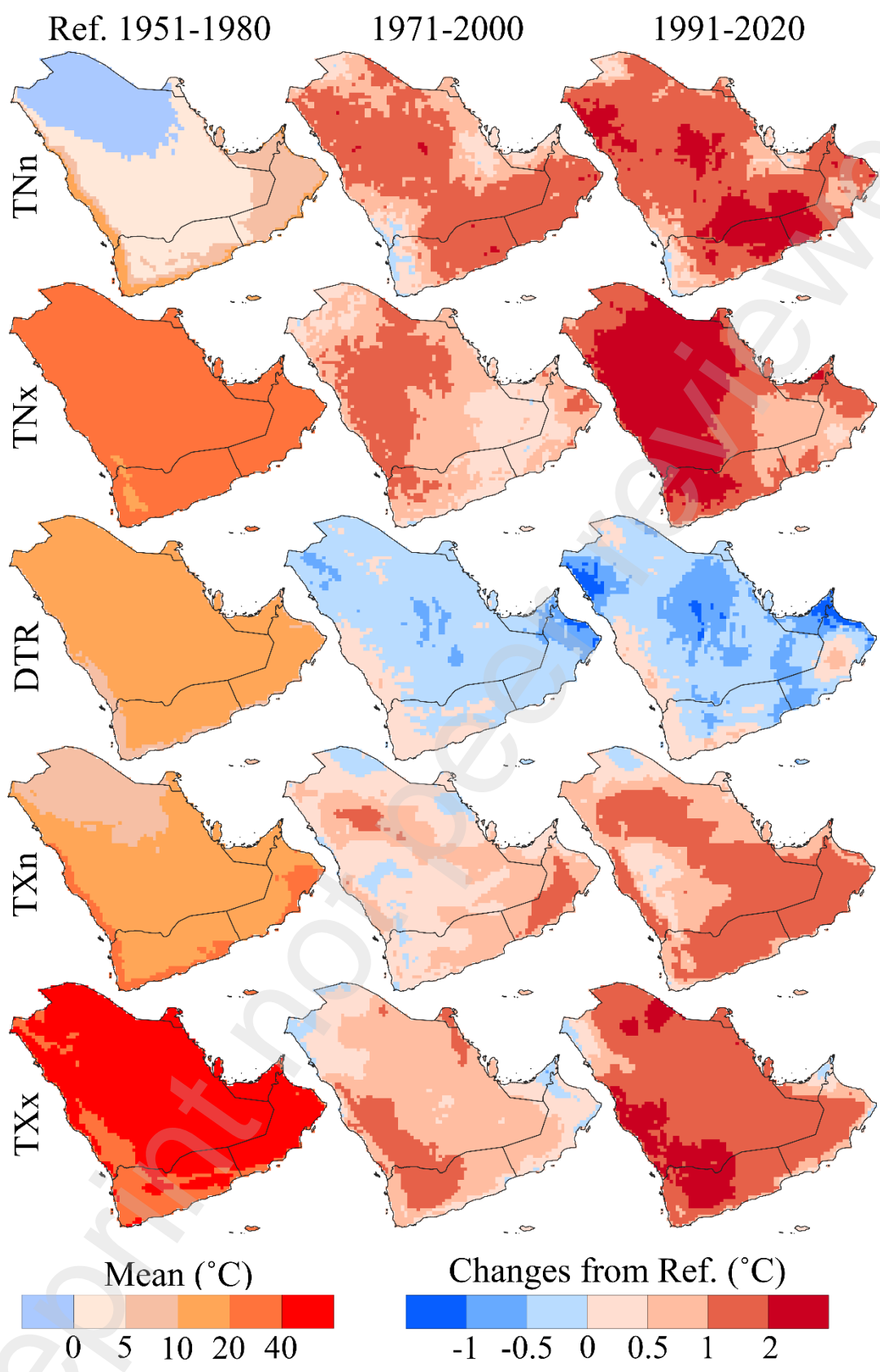
296 The spatial changes and temporal significant trends for the temperature (Absolute, Relative,
297 and Duration) and precipitation (Frequency and Intensity) sets of indices utilized in the present
298 research to describe the climate variability of TempPrec extremes across AP are explained in
299 the following sub-sections.

300

301 **4.1. Changes and Trends in Absolute Indices**

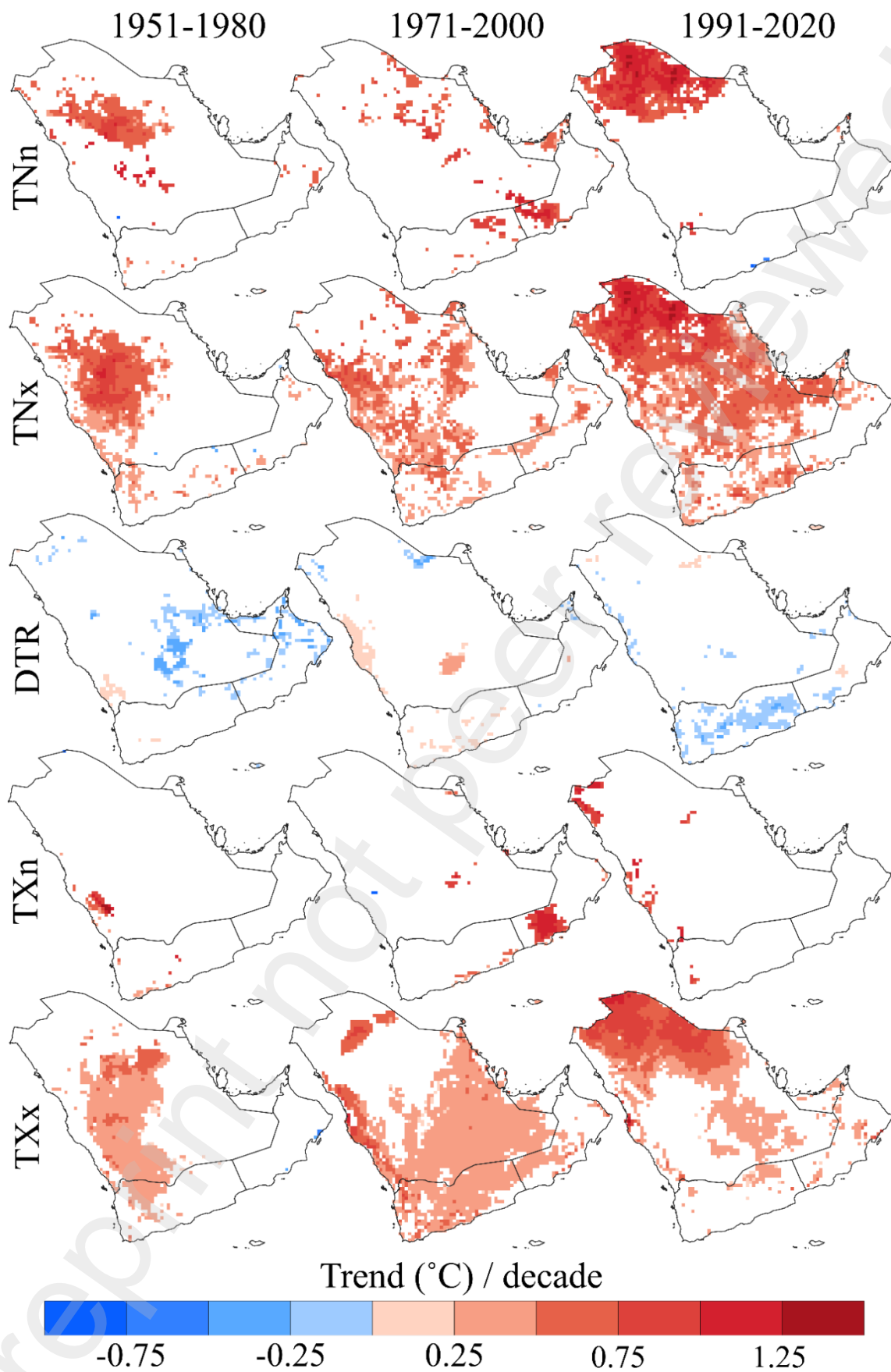
302 To understand the temperature variability in the AP, 30-year mean patterns of the annual time
303 scale for the Absolute Temperature Indices were analyzed and shown in **Fig. 3**, and the
304 temporal trends and their significance at $p < 0.05$ were calculated and shown in **Fig. 4**. The
305 utilization of reanalysis data offers a significant advantage by providing precise results for each
306 grid box within the area of interest. Generally, in compliance with previous studies on the AP,
307 warming patterns are well observed. The changes are gradually decreasing for DTR and
308 increasing for the rest of the absolute indices. Among the absolute indices, TXn, TXx, TNn,
309 and TNx are increasing overall AP areas, with some even displaying statistical significance
310 trends. Among the absolute indices, TNx exhibits the most significant change, with an increase
311 of greater than 3°C above the reference period. During the period 1991-2020, most of the
312 Kingdom of Saudi Arabia (KSA) and Yemen experienced a warming change of more than 2°C
313 in the maximum of the Tmin (TNx) index compared to the reference period. The DTR index is
314 decreasing gradually in most regions. The highest decreasing change ($> -1^\circ\text{C}$) was observed
315 over the UAE, the interior and northwest of KSA, and the highlands of north Oman during
316 1991-2020. This shows that the Tmin is rising slower than the Tmax, and maybe the Tmax is
317 rising quicker than the Tmin, or both are happening simultaneously.

318 The spatial distribution for the significant trends (p-value less than 0.05) is illustrated in
319 **Fig. 4** for all Absolute Temperature Indices for the three specified time frames, namely 1951-
320 1980, 1971-2000, and 1991-2020. During all defined periods, all absolute indices showed
321 significant increasing trends, except for the DTR index, where a few minor decreasing trends
322 are noticed in the Empty Quarter desert, northern Oman, and several parts of the UAE during
323 the first period, and a slight downward trend (-0.25°C per decade) covers most parts of Yemen
324 during the recent period. Between 1991 and 2020, a notable increasing trend of more than 1°C
325 per decade was observed in TNn, TNx, and TXx indices, particularly in the northern AP. The
326 trends in TXn during all periods are observed in limited areas but with higher magnitude.
327



328
329
330
331
332

Fig. 3. Spatial distribution of the Absolute Temperature Indices obtained from ERA5 reanalysis data. The left column represents the annual mean of the reference period (1951-1980), and the middle and right columns represent the changes (differences) from the reference period.



333

334 **Fig. 4.** Spatial pattern of the significance trends ($p < 0.05$) in Absolute Temperature Indices

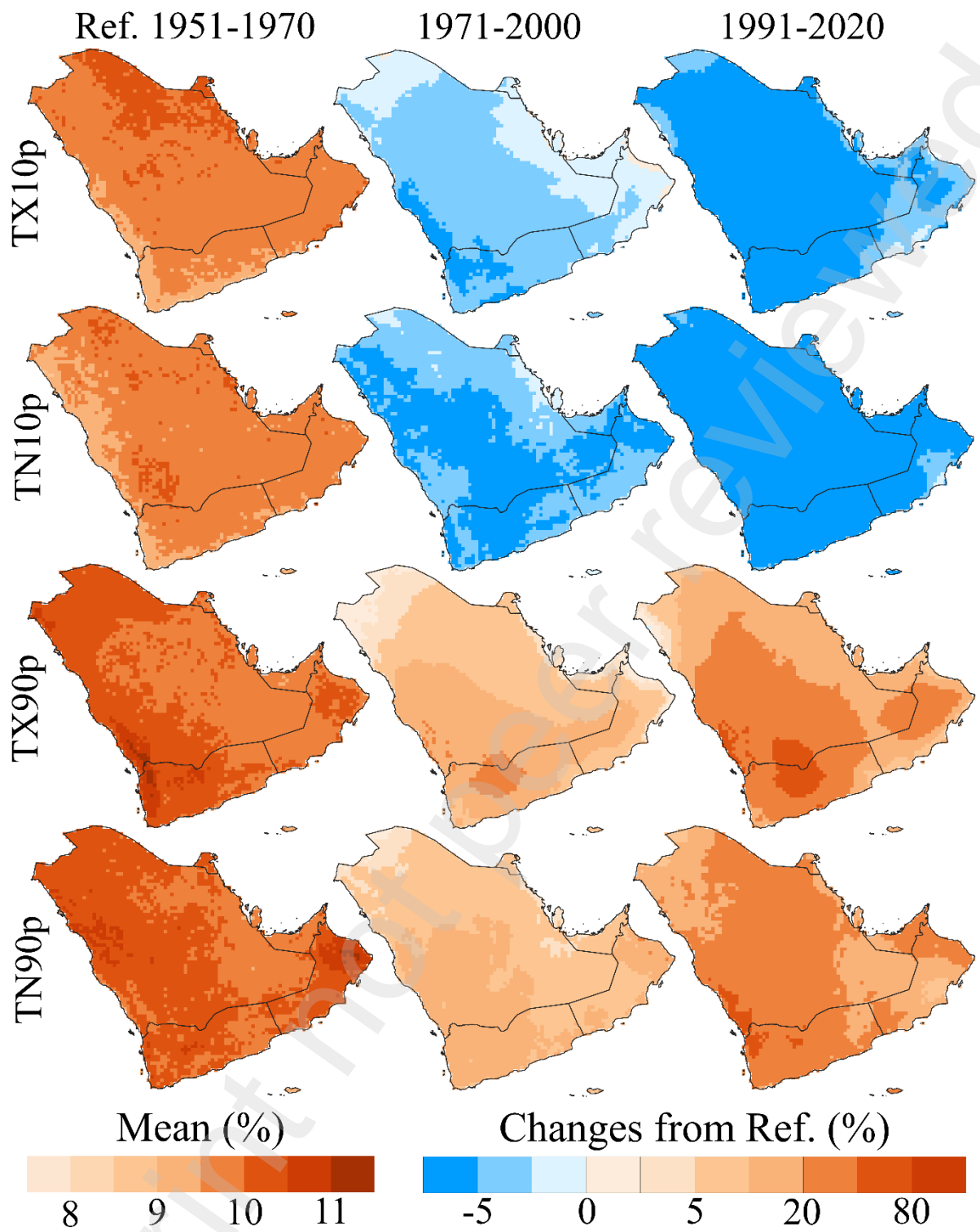
335 obtained from ERA5 for the three defined periods. The colors represent the rate of change.

336 4.1.1. Changes and Trends in Relative Indices

337 The changes in Relative Temperature Indices TN10p, TX90p, TN90p, and TX10p are
338 presented in **Fig. 5**. These indices are served to characterize changes in temperature extremes.
339 According to ETCCDI (2020), cool days (TX10p) indicate the proportion of days when the
340 T_{max} surpasses the tenth percentile. This represents the frequency of unusually cold days,
341 while cool nights (TN10p) mean the frequency of occasions when T_{min} falls below the 10th
342 percentile. This represents the frequency of unusually cold nights. **Fig. 5** shows a decreasing
343 change in both TN10p and TX10p throughout both recent periods, where a slower value
344 represents cold temperatures. During 1991-2020, most regions of the AP experienced
345 decreased cold days and nights by more than -5% than the reference period. Similarly, TX90p
346 (warm days) indicates the ratio of days when the highest recorded temperature surpasses the
347 90th percentile. This represents the frequency of unusually hot days, while TN90p (warm
348 nights) means the proportion of days when the T_{min} is under the tenth percentile. This
349 represents the frequency of unusually warm nights. Both TX90p and TN90p indices show a
350 gradually increasing change from the reference period during the recent study periods. The
351 highest change in TN90p (~50%) is located over the southwest highlands of Yemen and KSA,
352 while Yemen's north-central areas have shown the highest change (~50%) in TX90p. These
353 changes suggest that the climate is becoming warmer overall, with more warm extremes and
354 fewer cold extremes.

355 The significant trends ($p < 0.05$) for all Relative Indices are depicted in **Fig. 6**. From 1951
356 to 1980, significant declining trends in cool days (TX10p) were observed in the western regions
357 of the AP as well as in central Yemen. Similarly, the trends in cool nights (TN10p) exhibited
358 a decrease over the AP's northern and central regions. Conversely, increasing trends were
359 observed across all periods in the TX90p and TN90p indices. The highest trends in warm days
360 and nights were observed in the northern AP during 1991-2020. Additionally, there has been a
361 significant increasing trend in warm nights along the southern shores of Yemen recently.

362



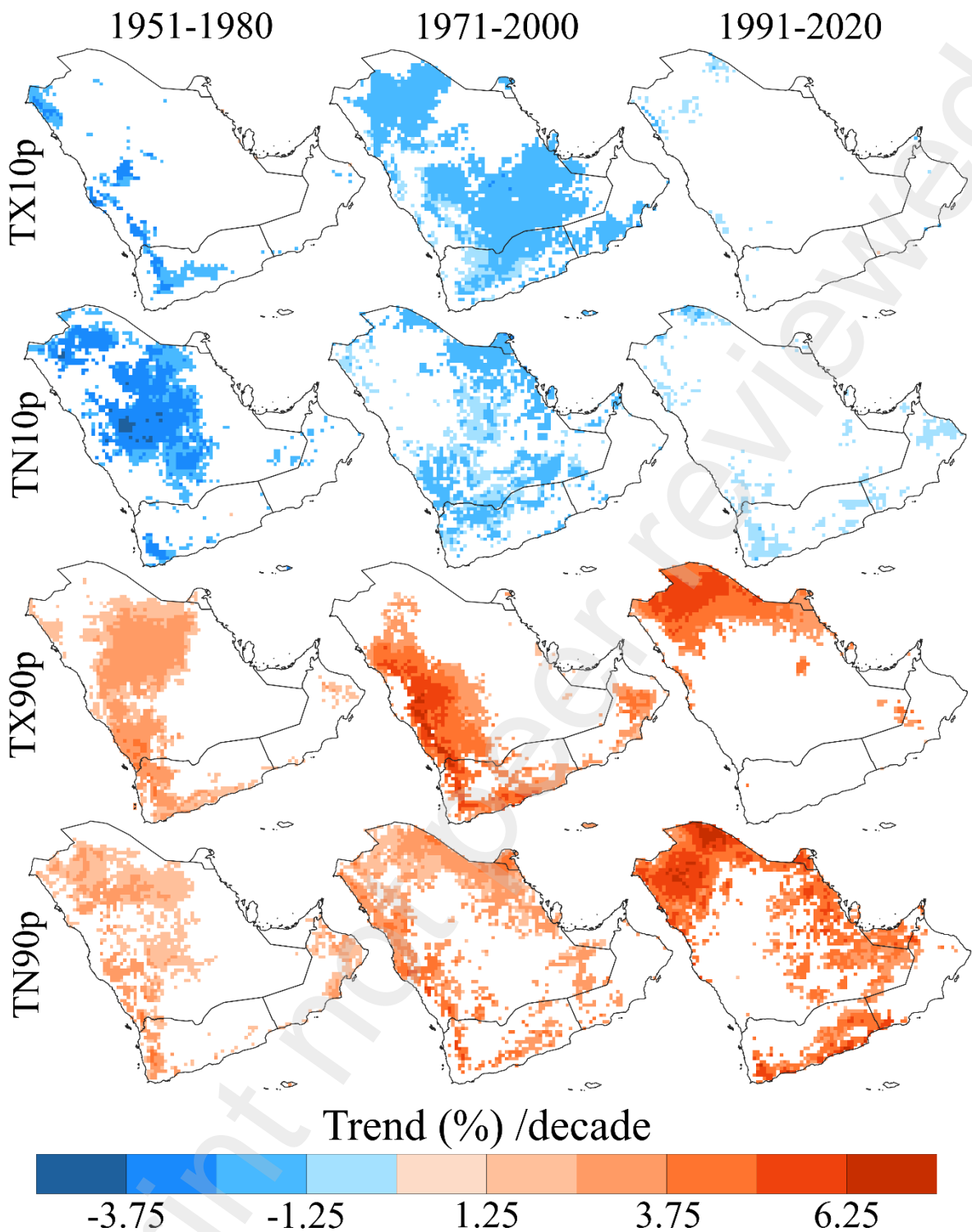
363

364

365

366

Fig. 5. Same as Fig. 3 but for Relative Temperature Indices.



367

368

369

370 4.1.2. Changes and Trends in Duration Indices

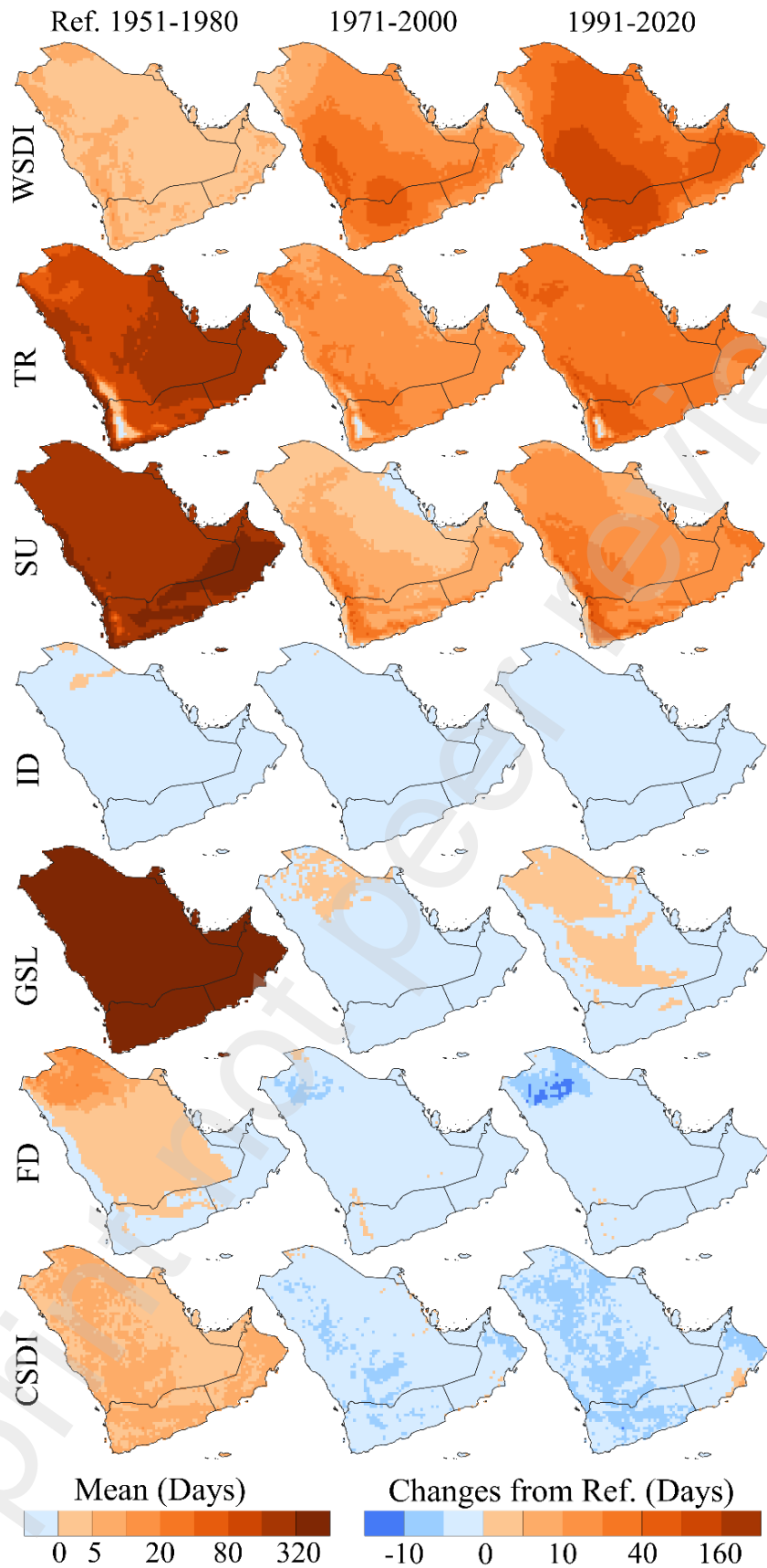
371 The changes in Duration Temperature Indices, including Ice days (ID), Warm Spell Duration

372 Indicator (WSDI), Frost days (FD), Tropical nights (TR), Growing Season Length (GSL),

373 Summer days (SU), and Cold Spell Duration Indicator (CSDI) are presented in **Fig. 7**. These
374 indices are used to determine changes in temperature duration. There is a dominant increasing
375 trend in the TR, SU, and WSDI indices across most of the AP for both recent periods compared
376 to the reference period. The highest change (80 days) of these indices is spread over the
377 highlands of KSA and Yemen. Increasing SU, TR, and WSDI indices in the AP indicate a
378 warming climate. This warming climate is characterized by more hot days, warmer nights, and
379 longer periods of sustained heat. The duration of the growing season, also known as GSL, is
380 determined by the time span between the initial and final instances when the temperature in a
381 year is sufficiently warm to support plant growth, which has increased lightly and gradually
382 over the northern and central KSA. Frost Days (FD) has a gradually decreasing change over
383 the northern AP during both recent periods regarding the reference period. A gradually
384 decreasing change in CSDI was observed for most of Yemen and KSA and over northern Oman
385 during both recent periods. The Ice Days (ID) index has almost no changes during both periods.
386 Most previous studies ignored the Growing Season Length (GSL), Frost Days (FD), and Ice
387 Days (ID) indices due to local climate characteristics (Almazroui, 2020b; Almazroui et al.,
388 2022; Alsarmi and Washington, 2014). However, ERA5 showed reasonably considered results
389 for GSL and FD indices over northern AP, as mentioned above.

390 The significant trends when $p < 0.05$ for all Duration Indices are presented in **Fig. 8** for
391 the three specific time frames. Generally, WSDI, TR, and SU have raised trends in overall
392 defined periods except for WSDI during 1951-1980 where it has increased and decreased
393 slightly. The highest observed trends were in WSDI over the AP's southwest highlands (22
394 days per decade) during 1971-2000 and over northern AP (20 days per decade) during 1991-
395 2020. GSL and ID didn't show any notable trends over all periods. Frost Days (FD) and CSDI
396 indices show scattered decreasing trends across several regions in AP. The lowest trend
397 decrease (6 days per decade) is observed over the north AP. Overall, these statistically
398 significant trends, i.e., the increases in SU, TR, and WSDI, along with the decreases in FD and
399 CSDI indices, suggest a clear warming trend in the AP.

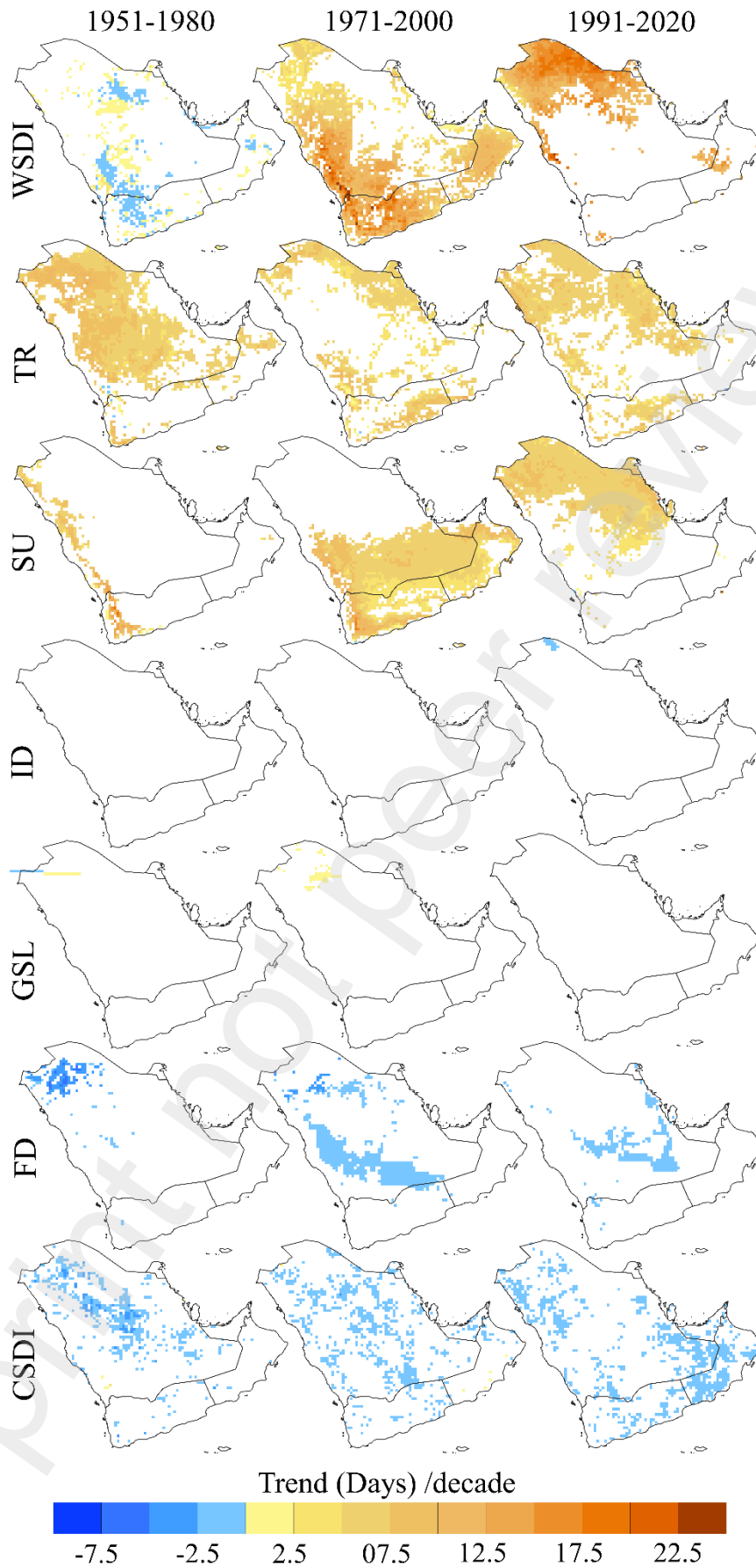
400



401

402

Fig. 7. Same as **Fig. 3** but for Duration Temperature Indices.



403

404

Fig. 8. Same as Fig. 4 but for Duration Temperature Indices.

405

406 **4.2. Changes and Trends in Intensity Indices**

407 Among the Intensity Precipitation Indices shown in **Fig. 9**, and according to ETCCDI (2020),
408 these indices capture specific facets of precipitation. The maximum 1-day/5-day precipitation
409 amount (RX1day/5day) indices focus on the duration and intensity of extreme rainfall events,
410 while R95pTOT and R99pTOT highlight the heavy and very heavy precipitation's contribution
411 to the total amount. PRCPTOT provides a measure of total precipitation, regardless of intensity.
412 The Simple Daily Intensity Index (SDII) describes the mean quantity of precipitation that
413 occurs on a wet day. The changes in the SDII index were observed to be relatively small,
414 indicating only modest shifts in daily precipitation intensity. However, Over the eastern areas,
415 there was a minor decrease in the SDII index during both periods, suggesting a slight reduction
416 in daily precipitation intensity. Conversely, the western regions exhibited a small increase in
417 the SDII index, indicating a slight upturn in daily precipitation intensity.

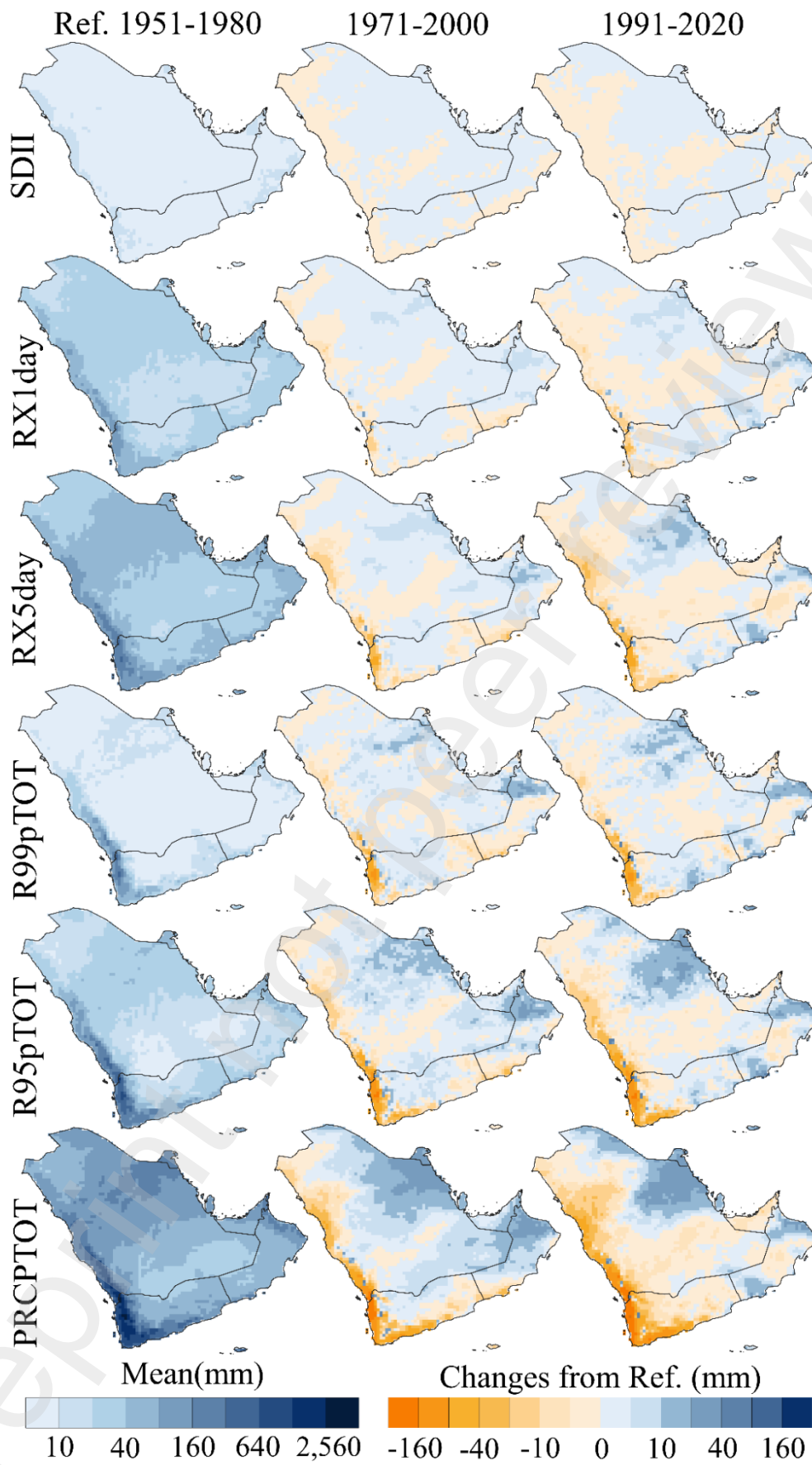
418 Maximum one-day precipitation (RX1day) represents the maximum amount of
419 precipitation in a single day. Similar to SDII, the western coastal areas have slightly and
420 gradually decreased RX1day over the two recent periods. This indicates a lower occurrence of
421 intense one-day precipitation incidents along these shorelines. At the same time, most other
422 areas of the AP have a slight but positive change in RX1day, including specific small regions
423 such as Al-Bahah and Abha in KSA, Salalah and northern Oman, heading towards a much
424 more intense single-day rainfall amount. The same applies to the RX5day index, which
425 represents the cumulative precipitation. It is also similar and gradual in change. The highest
426 positive change in the RX5day index (30mm) is located over the middle eastern regions of
427 Saudi Arabia, southern Kuwait, Al-Mukalla and Al-Ghaydah cites in the southern shoreline of
428 Yemen, and northern and southern Oman.

429 The R95/99pTOT (Precipitation from days exceeding the 95/99th percentile) indices
430 represent wet and extremely wet events, respectively. They show a gradual change, with a
431 negative change over the southwestern coasts of KSA and Yemen and a positive change over
432 several regions in the east regions. This indicates that there are more intense precipitation
433 events occurring in these regions. Southern Kuwait, central and eastern Saudi Arabia, Dhofar
434 province, and the northern mountainous ranges in Oman, including the capital city Muscat,
435 have recently received the highest precipitation (R95/99pTOT). The total rainfall amount
436 (PRCPTOT) is similar to R95/99pTOT. PRCPTOT has decreased in several regions during
437 both periods, leading to desertification or drought. At the country level, Qatar, Bahrain, and

438 Kuwait experienced a positive change in PRCPTOT during the last two periods, while the UAE
439 received less precipitation when compared to the reference period. Particular locations in the
440 southwestern highlands of KSA, as well as the eastern areas of KSA, and the northern and
441 southern parts of Oman, have experienced the highest changes in the PRCPTOT index during
442 the recent period. In Yemen, PRCPTOT has mostly decreased, except in the high western
443 mountain peaks, the highest in the AP (Peaklist.org, 2006), namely Jabal Al-Nabi Shuaib and
444 Jabal Al-Tayyal. Similar to RX1day, the city of Salalah in the Dhofar region has undergone a
445 noticeable positive change in precipitation amounts during the recent period, contrasting with
446 the previous period.

447 The statistically significant trends ($p < 0.05$) for all intensity indices are presented in **Fig.**
448 **10** for the three designated time frames. During all periods, all intensity indices except
449 PRCPTOT show a scattered negative trend over some areas of the AP. These decreasing trends
450 are gradual among the three time periods. There is a noticeable increasing trend located in
451 southern Kuwait during 1971-2000 and at the top northern AP during 1991-2020 in most
452 intensity indices. The highest decreasing trend (-160 mm per decade) in PRCPTOT is located
453 over parts of the southwestern highlands of the AP during the recent period.

454

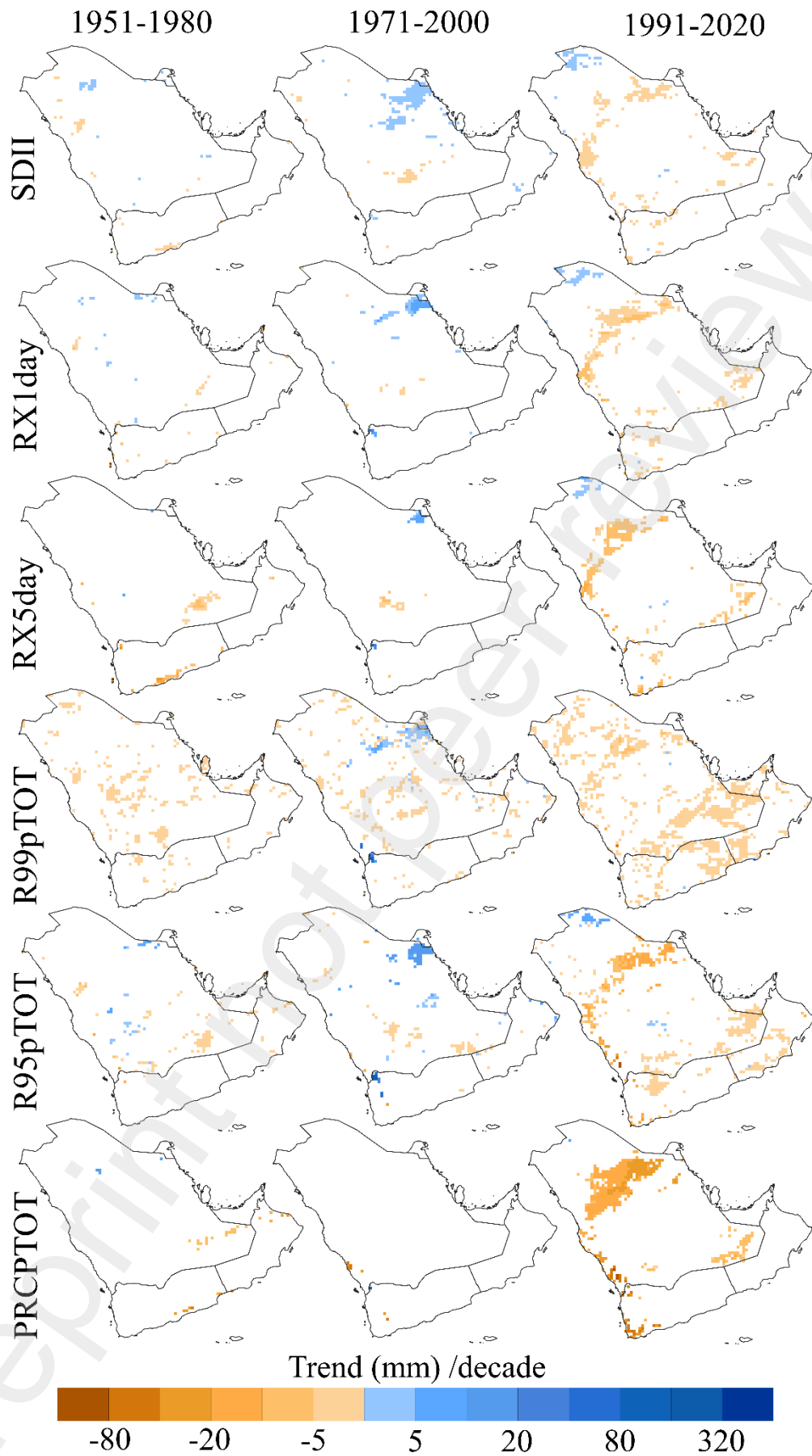


455

456

Fig. 9. Same as **Fig. 3** but for Intensity Precipitation Indices.

457



458

459

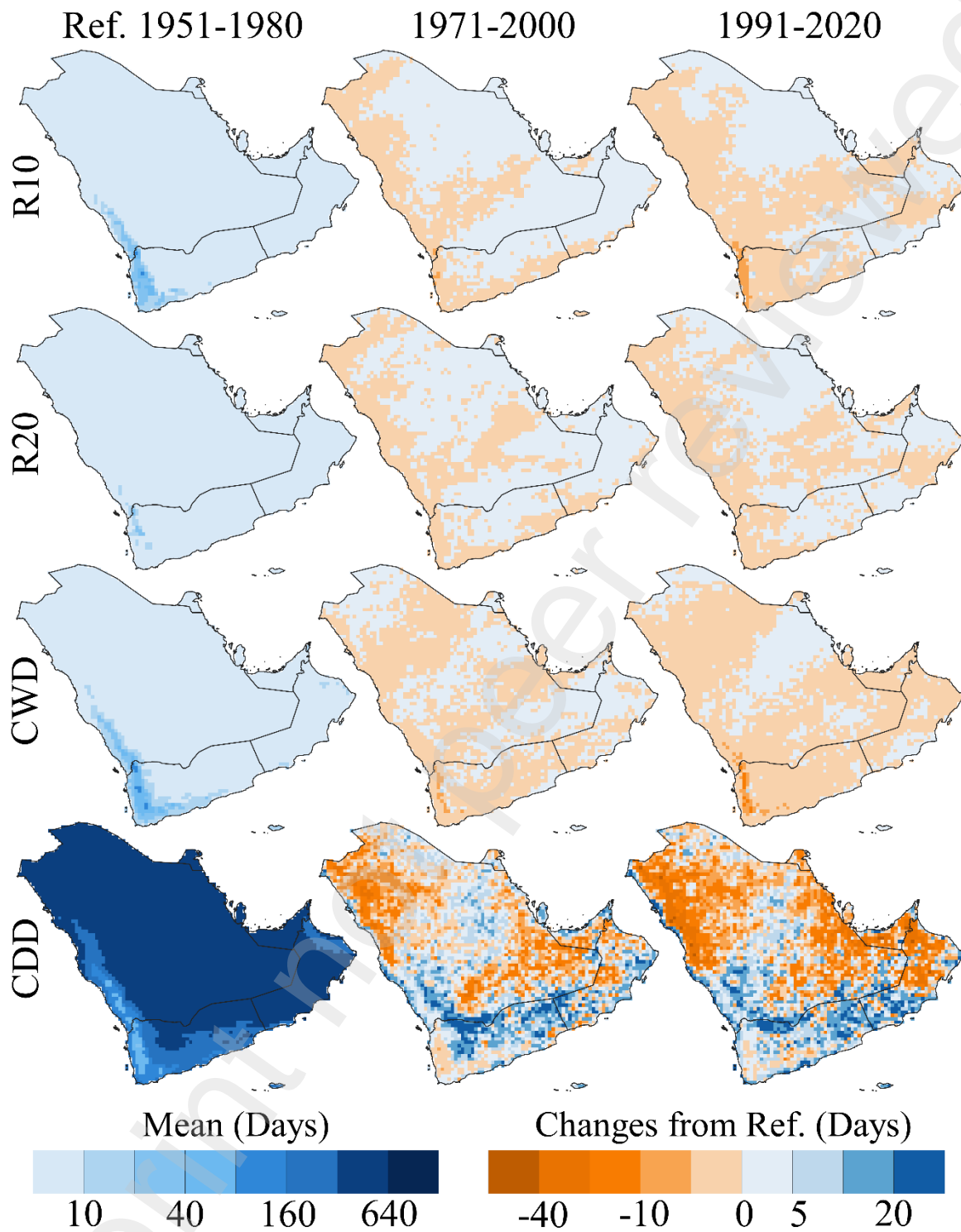
Fig. 10. Same as Fig. 4 but for Intensity Precipitation Indices.

460

461 **4.2.1. Changes and Trends in Frequency Indices**

462 Frequency Precipitation Indices shown in **Fig. 11** provide good insights into precipitation
463 magnitude. The changes in these indices were gradual from 1971-2000 to 1991-2020. Unlike
464 the RX1/5day indices, which focus on extreme precipitation events over a specific duration,
465 R10 and R20 are based on threshold exceedances regardless of duration. It can be observed
466 that heavy rainfall (R10) has slightly decreased in the western and southern areas of the AP,
467 while it has increased slightly in the eastern areas, except for the UAE, which experienced a
468 slight decrease in R10. The highest decrease was observed over the western highlands of
469 Yemen during 1991-2020 compared to the reference period. The Consecutive Wet Days
470 (CWD) index clearly depicts the Fertile western highlands within the reference period (1951-
471 1980). The changes in CWD are similar to R10 and R20. The highest decrease in CWD was
472 observed over the western highlands of Yemen during 1971-2000 and 1991-2020. The decrease
473 in CWD suggests a decline in continuous precipitation over time. The reduction in the duration
474 of precipitation may result in decreased water availability for agriculture, ecosystems, and
475 human consumption. It may result in water stress and affect the overall water resources in the
476 fertile regions of Yemen. Consecutive Dry Days (CDD) considers a threshold below which
477 precipitation is negligible or nonexistent. CDD dominates most of the AP during the reference
478 period, reflecting its climate. Changes in CDD are disparate among the grid boxes. The changes
479 seem to be gradual between 1971-2000 and 1981-2020. Parts of Saudi Arabia, Oman, Qatar,
480 Kuwait, and the UAE are heading towards a decrease in dry spells, in contrast to Yemen, where
481 more dry periods are trending. Moreover, Wet spells (CWD) decreased over Yemen recently.
482 Furthermore, Yemen has a higher predominant CDD index than other countries in the AP
483 during both recent periods, indicating that dry spells are more persistent and severe in Yemen.
484 Socotra, the largest and most important Yemeni island and one of the main tourist destinations
485 in Yemen, also has a high CDD value.

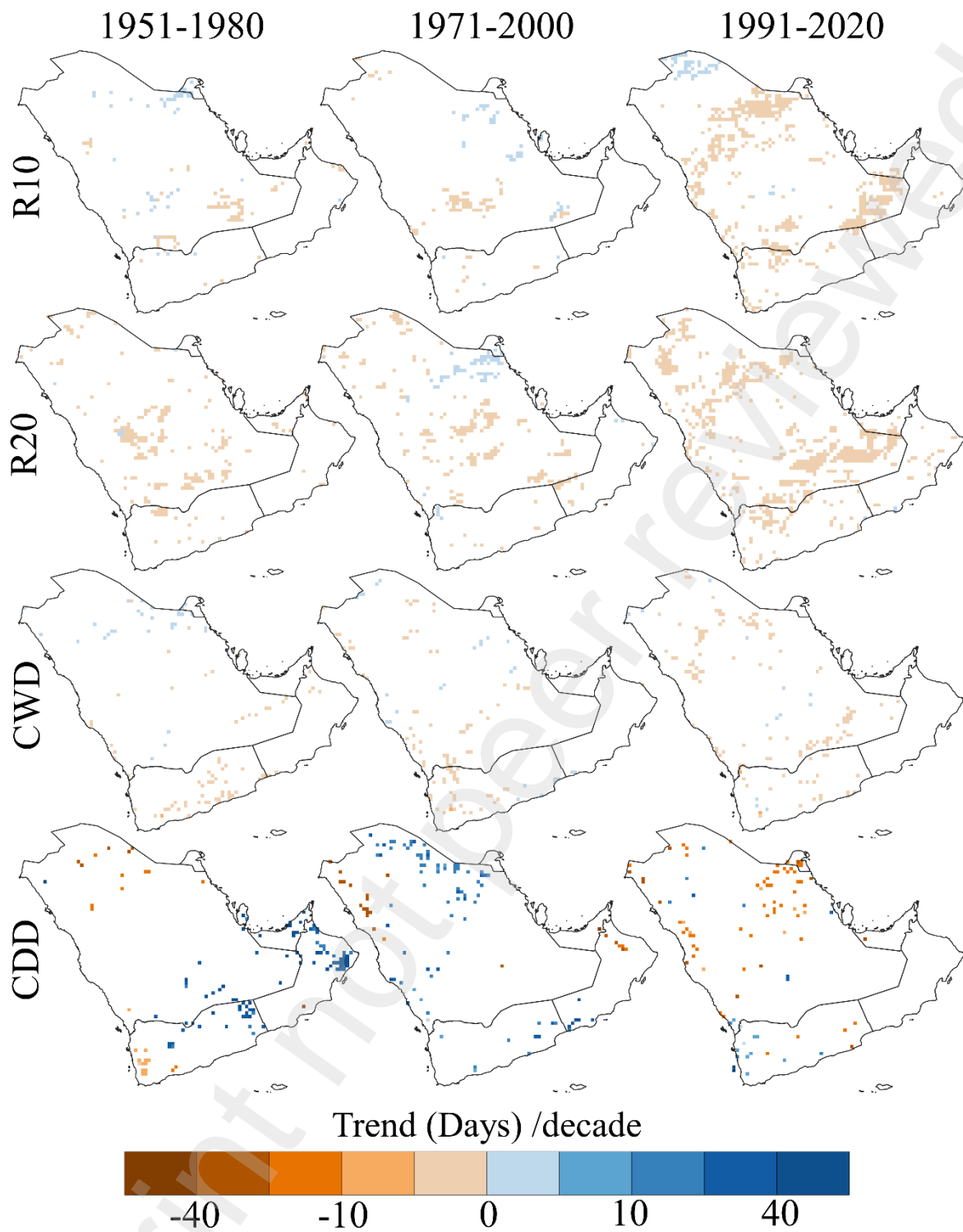
486 The trends (statistically at a significant level of $p < 0.05$) for all frequency indices are
487 presented in **Fig. 12** for the three defined periods. Overall, the trends in rainfall patterns are
488 scattered and observed over fewer grids across the AP. There are gradually decreasing trends
489 in heavy and very heavy rainfall (R10/20) during all periods in several parts of the AP. Most
490 trends in CWD are weak or non-significant, with the weak trend being negative. Similarly, the
491 trends in Consecutive Dry Days (CDD) demonstrate both fewer decreasing and increasing
492 trends over the AP during all periods.



494

495

Fig. 11. Same as Fig. 3 but for Frequency Precipitation Indices.



496

497

498

Fig. 12. Same as **Fig. 4** but for Frequency Precipitation Indices.

499 5. Discussion

500 Alexander et al. (2006) explained that there is still a lack of appropriate and reliable data for
501 monitoring climate changes, particularly climate extremes, in many regions, especially remote
502 areas. Despite being the second-largest country on the peninsula (AL-wesabi et al., 2022), data
503 from weather stations located in Yemen has been omitted from most previous studies in the
504 region. This may be due to the country's strict climate data-sharing policies (AL-Falahi et al.,
505 2020). To overcome these barriers, the present study aims to investigate the spatial distribution
506 along with temporal trends concerning extreme TempPrec indices throughout the AP
507 employing the indices suggested by ETCCDI using the ERA5 reanalysis data. The utilization
508 of reanalysis data offers a significant advantage by providing precise results for each single
509 grid box within the area of interest. This helped to highlight the affected areas accurately.
510 According to Lei et al. (2022), ERA5 was found to be a reliable dataset for analyzing
511 precipitation extremes in China, with a strong correlation between simulated and actual
512 precipitation data. For temperature, Xu et al. (2022) documented that ERA5 data are reliable
513 for simulating temperature data and identifying extreme temperature events. Velikou et al.
514 (2022) found that ERA5 performs well in replicating extreme temperatures even across Europe,
515 such as heatwaves and cold spells.

516 The findings of this paper's analysis of all temperature indices generally indicate a clear
517 warming trend across all parts of the AP. Extensive regions have experienced warming
518 exceeding the threshold of 2°C, with some areas even surpassing the 3°C threshold compared
519 to the reference period. The northern and northeastern regions recently experienced higher
520 warming rates in TNn, TNx, and TXx (>1°C per decade) than the rest of the AP. The Qaisumah
521 station in Saudi Arabia, recorded temperature breaks, with Tmax reaching 50.8°C in 2007
522 (Christidis et al., 2023). These warming patterns align with the outcomes of prior research
523 efforts carried out across AP utilizing station data (Alghamdi and Moore, 2014; Almazroui,
524 2020b; Almazroui et al., 2022, 2014; Alsarmi and Washington, 2014; Donat et al., 2014;
525 Odnoletkova and Patzek, 2021; Zhang et al., 2005). This highlights the reliability and
526 credibility of the ERA5 reanalysis data over AP (Odnoletkova and Patzek, 2021). Conversely,
527 Gunawardhana and Al-Rawas (2014) reported that TXx and TNn have decreased over Muscat,
528 Oman, during 1986-2011. However, our findings show no significant trends, higher positive
529 changes in TNn, and lower changes in TXx over Muscat during all periods.

530 Based on **Fig. 2** and **4**, it is evident that the Tmin has increased more than the Tmax.
531 As a result, the DTR trends and changes have decreased, consistent with prior research over

532 AP (Alghamdi and Moore, 2014; Almazroui, 2020b; Almazroui et al., 2022, 2014; Alsarmi
533 and Washington, 2014; Odnoletkova and Patzek, 2021) and globally (Sun et al., 2019).
534 However, the decreasing trends in DTR during the recent period are limited over Yemen (Fig.
535 4), possibly due to discrepancies in trend analysis methods. It is worth noting that Xu et al.
536 (2022) found that ERA5 did not accurately capture the trend of the DTR over China. The
537 changes in warm nights and days (TN90p/TX90p) are greater than the changes in cold nights
538 and days (TN10p/TX10p) from the reference period, agreeing with the prior investigation
539 (Almazroui, 2020b; Almazroui et al., 2014; Donat et al., 2014; Odnoletkova and Patzek, 2021).
540 This suggests that the region is experiencing more frequent and intense heatwave events. This
541 also suggests that extreme warm temperatures are becoming more common while extreme cold
542 temperatures are less prevalent. It implies a potential change in the overall temperature regime
543 of the region. The highest change, exceeding 80% compared to the reference period, is
544 observed in the areas along the shared borders between Yemen and Saudi Arabia. Duration
545 indices provided further evidence of a warming climate in the AP. Years without a cold wave
546 are more frequent than those without a heat wave, which are exceedingly rare.

547 Overall, the rise in temperature extremes will undoubtedly affect various environmental
548 sectors like energy production and water-related industries, agriculture, and service catering to
549 religious travellers. Furthermore, TempPrec extremes over AP may also have an impact due to
550 large-scale circulation and diversified topography (Abid et al., 2018; Almazroui et al., 2019;
551 Attada et al., 2019; Charabi, 2009; Donat et al., 2014; Rashid et al., 2020). According to the
552 findings of Donat et al. (2014), significant positive correlations were observed between the
553 Southern Oscillation Index (SOI) and DTR at various locations in the AP and northeast Africa.
554 Additionally, they noted that during La Niña seasons, the DTR tends to be higher than El Niño
555 seasons. Hamed et al. (2023a) reported that the populations in Saudi Arabia, the UAE, and
556 Qatar would be most affected by the change in temperature extremes. It is worth mentioning
557 that the central regions of Yemen and the southwestern regions of KSA have experienced the
558 most significant warm changes in compound TXX, TX90p, SU, TR, and WSDI indices
559 compared to the reference period. These compound changes demonstrate the severity of
560 extreme temperature events, such as heat waves, from which these regions suffer (Jiang et al.,
561 2023). To adapt to more frequent and intense heatwave events, these areas should undertake
562 measures including: 1) enhancing early warning systems for heatwaves; 2) providing cooling
563 centres and other services for people vulnerable to heat stress; 3) promoting water conservation
564 and efficiency measures; and 4) investing in renewable energy sources. More appropriate
565 strategies and summery for policy makers are discussed by Odnoletkova and Patzek (2021).

566 By taking these actions, these regions can better protect their populations and resources from
567 the impacts of future heatwave spells.

568 The spatial distributions of precipitation extremes throughout the AP have shown minor
569 and non-significant trends (**Fig. 10** and **12**) when compared to temperature extremes, which
570 aligns with the findings of most studies in the literature. The lack of clear trends in the AP's
571 precipitation might be related to the high temporal and spatial variability of precipitation within
572 a topographically diverse and arid environment (AlSarmi and Washington, 2011; Nasrallah
573 and Balling, 1996). By observing the changes in all rainfall indices shown in **Fig. 9** and **11**, a
574 noticeable shift in the spatial distribution of rainfall from the fertile western regions to the
575 eastern regions of the AP can be observed. This shift explains the recent increasing trend in
576 rainfall over Kuwait (Al-Qallaf et al., 2020) and eastern Saudi Arabia, especially Dammam
577 city (Almazroui, 2020c). The rainfall indices exhibit varied changes, with some regions
578 experiencing an increase while others experiencing a decline (Almazroui et al., 2012). During
579 1991-2020, all precipitation indices have shown small significant declining trends. Similar to
580 temperature findings, the spatial distributions and temporal trends of precipitation indices
581 revealed by this study are consistent with most prior research on the AP, which suggests the
582 credibility and validity of ERA5 reanalysis data in assessing climate extremes over the region.

583 In recent years, Oman has experienced an increasing susceptibility to heavy rainfall
584 events (Alimohammadi and Malakooti, 2018; Deshpande et al., 2010; Gunawardhana and Al-
585 Rawas, 2014). Specifically, the city of Salalah in Oman has seen simultaneous increase changes
586 in most intensity rainfall indices (RX1/5day, R95/99pTOT, and PRCPTOT) during the recent
587 period, as opposed to 1971-2000 when compared to the reference period. This is consistent
588 with the recent hurricanes that have hit the city (EM-DAT, 2023; FloodList, 2023; Mansour,
589 2019). Similarly, several other regions in the AP have been affected by compound intensity
590 rainfall indices, including RX1/5day, R95/99pTOT, and PRCPTOT. These regions include the
591 northern and southern coasts of Oman, the central and eastern regions of KSA, the highlands
592 of southwestern AP, southern Kuwait, and Socotra Island in Yemen (**Fig. 9**). Therefore, more
593 attention should be directed towards flood planning in these regions, including efforts to 1)
594 enhance drainage systems, construct flood barriers, and implement proper urban planning; 2)
595 improve early warning systems by investing in advanced meteorological technologies, such as
596 weather radar and automated monitoring stations; 3) strengthen emergency preparedness and
597 response; 4) raise public awareness; 5) create floodplain zoning; and 6) construct levees and
598 dams. The combination of higher values of the CDD index and lower values of the PRCPTOT
599 and CWD indices presents a clear indication of drought. This combination of indices is

600 observed concurrently in Yemen during both periods, signalling the presence of impending dry
601 spells that require careful consideration. To achieve that, several steps must be taken, including
602 1) stopping the fighting and promoting peace and stability; without peace, there can be no hope
603 for a sustainable future; 2) providing funding for water conservation and rainwater harvesting
604 projects; and 3) promoting drought-resistant crops. Yemen is extremely vulnerable to climate
605 change and its impacts, and the ongoing conflicts have made it difficult to respond to them
606 (Schulman, 2021).

607 The uniqueness of this study manifests in its innovative methodological approach. This
608 research moves beyond using limited station data from specific locations, a common limitation
609 in previous studies. Instead, it leverages ERA5 reanalysis data across the entirety of the AP,
610 offering a more comprehensive overview of the regional climate. Unlike most or all prior
611 studies that employed the MK method to investigate trends alone, this study utilizes the
612 superior MMK method. Moreover, the study broadened its analysis to cover changes from the
613 reference period. Furthermore, the study stands out in its temporal scope, spanning seven
614 decades, further subdivided into three distinct periods. This expansive timeframe and detailed
615 segmentation allow for a nuanced understanding of climate change over the AP.

616

617 **6. Conclusion**

618 Studying climate extremes in the AP is essential for understanding the potential impacts of
619 climate change on the region and informing adaptation and mitigation strategies. In order to
620 address the limited availability of local in situ data and policies across the AP, this study made
621 use of ERA5 reanalysis data to examine the spatial patterns and temporal trends of the
622 ETCCDI-defined extreme TempPrec indices within the AP between 1951 and 2020. The
623 analysis concluded a common warming trend across the AP, with most of them being
624 statistically significant. Warm extremes, which include warm nights and days, have gotten
625 more severe and frequent, alongside the duration of warm spells has also increased in most
626 regions. Conversely, cold extremes have declined, suggesting an accelerating warming trend.
627 The warming change (trend) exceeded the threshold of 2°C (1°C/decade⁻¹) in many regions,
628 indicating a rapid rate of temperature increase. This aligns with the results of previous research
629 and underscores the reliability of the ERA5 reanalysis data. Warming trends in temperature
630 indices will likely impact environmental sectors, including agriculture, water resources, and
631 sectors that provide services to religious travellers.

632 Regarding precipitation, rainfall indices indicate a shift in rainfall patterns from the
633 AP's fertile southwest regions towards more intense patterns in specific eastern regions,
634 including Oman, Kuwait, KSA, and Yemen. The temporal trends are weak in magnitude and
635 variable spatially, with dominant decreases in both intensity indices (-10 mm per decade) and
636 frequency indices (-5 days per decade). This indicates a shift towards more short, intense
637 rainfall events with longer dry periods in between, necessitating attention to flood and drought
638 planning. Conversely, Yemen encounters reduced rainfall amounts, leading to drought. These
639 findings emphasize the need to account for the observed trends in climate extremes when
640 planning for the future in the AP region. This study recommends:

- 641 1. Drought risks in Yemen are rising, calling for urgent implementation of adaptation
642 strategies in water resource management and agriculture.
- 643 2. Parts of Oman, Yemen, and Saudi Arabia should invest in flood prevention and
644 management to limit potential impacts.
- 645 3. Proactive adaptation is crucial as the AP experiences widespread warming, exceeding 2°C
646 temperature increases.
- 647 4. Climate variability must be considered in long-term water, agriculture, and urban
648 development planning.
- 649 5. Continuous monitoring using other reanalysis data, such as the Climate Forecast System
650 Reanalysis (CSFR) and Modern-Era Retrospective Analysis for Research and Applications
651 (MERRA-2). This can provide valuable insights into regional climate trends and support
652 evidence-based decision-making.

653 Further work is needed to investigate the region's Compound Drought and Heatwave
654 CDHW events. The above recommendations aim to guide future research on areas requiring
655 attention and action.

656

657 **Acknowledgement**

658 The authors greatly appreciate the University of Chinese Academy of Sciences (UCAS) for
659 providing a favorable working environment and technological support for conducting the
660 research. The authors would like to express gratitude to the European Centre for Medium-
661 Range Weather Forecasts (ECMWF) for generously providing the ERA5 dataset publicly
662 available. The first author acknowledges the "Alliance of International Science Organizations
663 (ANSO) Scholarship for Young Talents" for providing financial support for the academic study.
664 Grateful thanks are extended to Mohammed Saeed Hamid, Mohammed Alboory, and

665 Mohammed Hameed Ali Hizam from the Yemen Meteorological Services (YMS) for their
666 valuable support and encouragement. This work is jointly funded by National Natural Science
667 Foundation of China (No. 42071425), the CAS Strategic Priority Research Program (No.
668 XDA19030402), and Natural Science Foundation of China (No. ZR2017ZB0422).

669

670 **Data availability**

671 The ERA5 reanalysis data (ERA5 hourly data on single levels from 1940 to the present) can
672 be downloaded freely from the link:
673 <https://cds.climate.copernicus.eu/cdsapp#!/dataset/reanalysis-era5-single-levels?tab=form>

674

675 **CRedit authorship contribution statement**

676 **Ali Salem Al-Sakkaf:** Conceptualization, Methodology, Software, Writing –original draft,
677 Visualization, Investigation. **Jiahua Zhang:** Funding acquisition, Supervision. **Fengmei Yao:**
678 Conceptualization, Funding acquisition, Writing – review & editing, Supervision. **Mohammed**
679 **Magdy Hamed:** Methodology, Software, Writing – review & editing, preparation. **Claudien**
680 **Habimana Simbi:** Writing – review & editing. **Arslan Ahmed:** Writing – review & editing.
681 **Shamsuddin Shahid:** Software, Writing – review & editing. All authors have read and agreed
682 to the published version of the manuscript.

683

684 **Declaration of Competing Interest**

685 The authors declare that they have no known competing financial interests or personal
686 relationships that could have appeared to influence the work reported in this paper.

687

688

689

690

691

692

693

694

695 References

- 696 Abid, M.A., Almazroui, M., Kucharski, F., O'Brien, E., Yousef, A.E., 2018. ENSO relationship to
697 summer rainfall variability and its potential predictability over Arabian Peninsula region.
698 NPJ Clim Atmos Sci 1, 1–7. <https://doi.org/10.1038/s41612-017-0003-7>
- 699 Ahmed, K., Shahid, S., Chung, E., Ismail, T., Wang, X., 2017. Spatial distribution of secular
700 trends in annual and seasonal precipitation over Pakistan. *Clim Res* 74, 95–107.
701 <https://doi.org/10.3354/cr01489>
- 702 Aker, Ş.L., Aghaei, I., 2019. Comparison of Business Environments in Oil-Rich MENA Countries:
703 A Clustering Analysis of Economic Diversification and Performance. *Emerging Markets*
704 *Finance and Trade* 55, 2871–2885. <https://doi.org/10.1080/1540496X.2018.1537185>
- 705 Alexander, L. V., Zhang, X., Peterson, T.C., Caesar, J., Gleason, B., Klein Tank, A.M.G., Haylock,
706 M., Collins, D., Trewin, B., Rahimzadeh, F., Tagipour, A., Rupa Kumar, K., Revadekar, J.,
707 Griffiths, G., Vincent, L., Stephenson, D.B., Burn, J., Aguilar, E., Brunet, M., Taylor, M.,
708 New, M., Zhai, P., Rusticucci, M., Vazquez-Aguirre, J.L., 2006. Global observed changes
709 in daily climate extremes of temperature and precipitation. *J Geophys Res* 111, D05109.
710 <https://doi.org/10.1029/2005JD006290>
- 711 AL-Falahi, A.H., Saddique, N., Spank, U., Gebrechorkos, S.H., Bernhofer, C., 2020. Evaluation
712 the Performance of Several Gridded Precipitation Products over the Highland Region of
713 Yemen for Water Resources Management. *Remote Sens (Basel)* 12, 2984.
714 <https://doi.org/10.3390/rs12182984>
- 715 Alghamdi, A.S., Moore, T.W., 2014. Analysis and Comparison of Trends in Extreme
716 Temperature Indices in Riyadh City, Kingdom of Saudi Arabia, 1985–2010. *Journal of*
717 *Climatology* 2014, 1–10. <https://doi.org/10.1155/2014/560985>
- 718 Ali, Z., Hamed, M.M., Muhammad, M.K.I., Iqbal, Z., Shahid, S., 2023. Performance evaluation
719 of CMIP6 GCMs for the projections of precipitation extremes in Pakistan. *Clim Dyn.*
720 <https://doi.org/10.1007/s00382-023-06831-6>
- 721 Alimohammadi, M., Malakooti, H., 2018. Sensitivity of simulated cyclone Gonu intensity and
722 track to variety of parameterizations: Advanced hurricane WRF model application.
723 *Journal of Earth System Science* 127, 41. <https://doi.org/10.1007/s12040-018-0941-4>
- 724 Almazroui, M., 2020a. Changes in Temperature Trends and Extremes over Saudi Arabia for the
725 Period 1978-2019. *Advances in Meteorology* 2020.
726 <https://doi.org/10.1155/2020/8828421>
- 727 Almazroui, M., 2020b. Changes in Temperature Trends and Extremes over Saudi Arabia for the
728 Period 1978-2019. *Advances in Meteorology* 2020.
729 <https://doi.org/10.1155/2020/8828421>
- 730 Almazroui, M., 2020c. Rainfall trends and extremes in Saudi Arabia in recent decades.
731 *Atmosphere (Basel)* 11. <https://doi.org/10.3390/atmos11090964>
- 732 Almazroui, M., Halwani, H.A., Islam, Md.N., Ghulam, A.B.S., Hantoush, A.S., 2022. Regional
733 and seasonal variation of climate extremes over Saudi Arabia: observed evidence for the
734 period 1978–2021. *Arabian Journal of Geosciences* 15, 1605.
735 <https://doi.org/10.1007/s12517-022-10882-0>

- 736 Almazroui, M., Islam, M.N., Dambul, R., Jones, P.D., 2014. Trends of temperature extremes in
737 Saudi Arabia. *International Journal of Climatology* 34, 808–826.
738 <https://doi.org/10.1002/joc.3722>
- 739 Almazroui, M., Islam, M.N., Saeed, F., Alkhalaf, A.K., Dambul, R., 2017. Assessing the
740 robustness and uncertainties of projected changes in temperature and precipitation in
741 AR5 Global Climate Models over the Arabian Peninsula. *Atmos Res* 194, 202–213.
742 <https://doi.org/10.1016/j.atmosres.2017.05.005>
- 743 Almazroui, M., Nazrul Islam, M., Athar, H., Jones, P.D., Rahman, M.A., 2012. Recent climate
744 change in the Arabian Peninsula: Annual rainfall and temperature analysis of Saudi
745 Arabia for 1978-2009. *International Journal of Climatology* 32, 953–966.
746 <https://doi.org/10.1002/joc.3446>
- 747 Almazroui, M., Rashid, I.U., Saeed, S., Islam, M.N., 2019. ENSO influence on summer
748 temperature over Arabian Peninsula: role of mid-latitude circulation. *Clim Dyn* 53, 5047–
749 5062. <https://doi.org/10.1007/s00382-019-04848-4>
- 750 Almazroui, M., Saeed, S., 2020. Contribution of extreme daily precipitation to total rainfall
751 over the Arabian Peninsula. *Atmos Res* 231, 104672.
752 <https://doi.org/10.1016/j.atmosres.2019.104672>
- 753 Al-Mutairi, M., Labban, A., Abdeldym, A., Alkhouly, A., Abdel Basset, H., Morsy, M., 2023.
754 Diagnostic Study of a Severe Dust Storm over North Africa and the Arabian Peninsula.
755 *Atmosphere (Basel)* 14, 196. <https://doi.org/10.3390/atmos14020196>
- 756 Al-Qallaf, H., Aliewi, A., Abdulhadi, A., 2020. Assessment of the effect of extreme rainfall
757 events on temporal rainfall variability in Kuwait. *Arabian Journal of Geosciences* 13,
758 1129. <https://doi.org/10.1007/s12517-020-06086-z>
- 759 Alriah, M.A.A., Bi, S., Nkuzimana, A., Elameen, A.M., Sarfo, I., Ayugi, B., 2022. Multiple
760 gridded-based precipitation products' performance in Sudan's different topographical
761 features and the influence of the Atlantic Multidecadal Oscillation on rainfall variability
762 in recent decades. *International Journal of Climatology* 42, 9539–9566.
763 <https://doi.org/10.1002/joc.7845>
- 764 AlSarmi, S., Washington, R., 2011. Recent observed climate change over the Arabian
765 Peninsula. *Journal of Geophysical Research Atmospheres* 116, 1–15.
766 <https://doi.org/10.1029/2010JD015459>
- 767 AlSarmi, S.H., Washington, R., 2014. Changes in climate extremes in the Arabian Peninsula:
768 Analysis of daily data. *International Journal of Climatology* 34, 1329–1345.
769 <https://doi.org/10.1002/joc.3772>
- 770 AL-wesabi, I., Zhijian, F., Bosah, C.P., Dong, H., 2022. A review of Yemen's current energy
771 situation, challenges, strategies, and prospects for using renewable energy systems.
772 *Environmental Science and Pollution Research* 29, 53907–53933.
773 <https://doi.org/10.1007/s11356-022-21369-6>
- 774 Arshad, M., Ma, X., Yin, J., Ullah, W., Liu, M., Ullah, I., 2021. Performance evaluation of ERA-5,
775 JRA-55, MERRA-2, and CFS-2 reanalysis datasets, over diverse climate regions of
776 Pakistan. *Weather Clim Extrem* 33, 100373.
777 <https://doi.org/10.1016/j.wace.2021.100373>

- 778 Attada, R., Dasari, H.P., Parekh, A., Chowdary, J.S., Langodan, S., Knio, O., Hoteit, I., 2019. The
779 role of the Indian Summer Monsoon variability on Arabian Peninsula summer climate.
780 *Clim Dyn* 52, 3389–3404. <https://doi.org/10.1007/s00382-018-4333-x>
- 781 Avila-Diaz, A., Bromwich, D.H., Wilson, A.B., Justino, F., Wang, S.-H., 2021. Climate Extremes
782 across the North American Arctic in Modern Reanalyses. *J Clim* 34, 2385–2410.
783 <https://doi.org/10.1175/JCLI-D-20-0093.1>
- 784 Bawadekji, A., Tonbol, K., Ghazouani, N., Becheikh, N., Shaltout, M., 2022. Recent atmospheric
785 changes and future projections along the Saudi Arabian Red Sea Coast. *Sci Rep* 12, 160.
786 <https://doi.org/10.1038/s41598-021-04200-z>
- 787 Bhatti, A.S., Wang, G., Ullah, W., Ullah, S., Hagan, D.F.T., Noon, I.K., Lou, D., Ullah, I., 2020.
788 Trend in extreme precipitation indices based on long term in situ precipitation records
789 over Pakistan. *Water (Switzerland)* 12, 1–19. <https://doi.org/10.3390/w12030797>
- 790 Charabi, Y., 2009. Arabian summer monsoon variability: Teleconexion to ENSO and IOD. *Atmos*
791 *Res* 91, 105–117. <https://doi.org/10.1016/j.atmosres.2008.07.006>
- 792 Christidis, N., Mitchell, D., Stott, P.A., 2023. Rapidly increasing likelihood of exceeding 50 °C in
793 parts of the Mediterranean and the Middle East due to human influence. *NPJ Clim Atmos*
794 *Sci* 6. <https://doi.org/10.1038/s41612-023-00377-4>
- 795 David Bronaugh, 2020. climdex.psic: PCIC Implementation of Climdex Routines [WWW
796 Document]. the Pacific Climate Impacts Consortium, R package version 1.1-11. URL
797 <https://CRAN.R-project.org/package=climdex.psic> (accessed 7.15.23).
- 798 Deshpande, M., Pattnaik, S., Salvekar, P.S., 2010. Impact of physical parameterization schemes
799 on numerical simulation of super cyclone Gonu. *Natural Hazards* 55, 211–231.
800 <https://doi.org/10.1007/s11069-010-9521-x>
- 801 Donat, M.G., Peterson, T.C., Brunet, M., King, A.D., Almazroui, M., Kolli, R.K., Boucherf, D., Al-
802 Mulla, A.Y., Nour, A.Y., Aly, A.A., Nada, T.A.A., Semawi, M.M., Al Dashti, H.A., Salhab,
803 T.G., El Fadli, K.I., Muftah, M.K., Dah Eida, S., Badi, W., Driouech, F., El Rhaz, K., Abubaker,
804 M.J.Y., Ghulam, A.S., Erayah, A.S., Mansour, M. Ben, Alabdouli, W.O., Al Dhanhani, J.S.,
805 Al Shekaili, M.N., 2014. Changes in extreme temperature and precipitation in the Arab
806 region: long-term trends and variability related to ENSO and NAO. *International Journal*
807 *of Climatology* 34, 581–592. <https://doi.org/10.1002/joc.3707>
- 808 Dubache, G., Asmerom, B., Ullah, W., Ogwang, B.A., Amiraslani, F., Weijun, Z., Gul, C., 2021.
809 Testing the accuracy of high-resolution satellite-based and numerical model output
810 precipitation products over Ethiopia. *Theor Appl Climatol* 146, 1127–1142.
811 <https://doi.org/10.1007/s00704-021-03783-x>
- 812 Easterling, D.R., Meehl, G.A., Parmesan, C., Changnon, S.A., Karl, T.R., Mearns, L.O., 2000.
813 Climate Extremes: Observations, Modeling, and Impacts. *Science* (1979) 289, 2068–
814 2074. <https://doi.org/10.1126/science.289.5487.2068>
- 815 EM-DAT, 2023. The international disaster database [WWW Document]. Centre for Research
816 on the Epidemiology of Disasters (CRED). URL <https://emdat.be/> (accessed 7.21.23).
- 817 ETCCDI, 2020. ETCCDI Climate Change Indices [WWW Document]. URL
818 <http://etccdi.pacificclimate.org/index.shtml> (accessed 6.20.23).

- 819 Fischer, E.M., Sippel, S., Knutti, R., 2021. Increasing probability of record-shattering climate
820 extremes. *Nat Clim Chang* 11, 689–695. <https://doi.org/10.1038/s41558-021-01092-9>
- 821 FloodList, 2023. Floods and flooding news from around the world [WWW Document]. URL
822 <https://floodlist.com/> (accessed 7.21.23).
- 823 Fonseca, R., Francis, D., Nelli, N., Thota, M., 2022. Climatology of the heat low and the
824 intertropical discontinuity in the Arabian Peninsula. *International Journal of Climatology*
825 42, 1092–1117. <https://doi.org/10.1002/joc.7291>
- 826 Francis, D., Chaboureaud, J.-P., Nelli, N., Cuesta, J., Alshamsi, N., Temimi, M., Pauluis, O., Xue,
827 L., 2021. Summertime dust storms over the Arabian Peninsula and impacts on radiation,
828 circulation, cloud development and rain. *Atmos Res* 250, 105364.
829 <https://doi.org/10.1016/j.atmosres.2020.105364>
- 830 Frich, P., Alexander, L., Della-Marta, P., Gleason, B., Haylock, M., Klein Tank, A., Peterson, T.,
831 2002. Observed coherent changes in climatic extremes during the second half of the
832 twentieth century. *Clim Res* 19, 193–212. <https://doi.org/10.3354/cr019193>
- 833 Giazzi, M., Peressutti, G., Cerri, L., Fumi, M., Riva, I.F., Chini, A., Ferrari, G., Cioni, G., Franch,
834 G., Tartari, G., Galbiati, F., Condemi, V., Ceppi, A., 2022. Meteonetwork: An Open
835 Crowdsourced Weather Data System. *Atmosphere (Basel)* 13, 928.
836 <https://doi.org/10.3390/atmos13060928>
- 837 Golshani, A., Banan-Dallalian, M., Shokatian-Beiragh, M., Samiee-Zenoozian, M., Sadeghi-
838 Esfahlani, S., 2022. Investigation of Waves Generated by Tropical Cyclone Kyarr in the
839 Arabian Sea: An Application of ERA5 Reanalysis Wind Data. *Atmosphere (Basel)* 13, 1914.
840 <https://doi.org/10.3390/atmos13111914>
- 841 Gunawardhana, L.N., Al-Rawas, G.A., 2014. Trends in extreme temperature and precipitation
842 in Muscat, Oman, in: *IAHS-AISH Proceedings and Reports*. IAHS Press, pp. 57–63.
843 <https://doi.org/10.5194/piahs-364-57-2014>
- 844 Gunawardhana, L.N., Al-Rawas, G.A., Kwarteng, A.Y., Al-Wardy, M., Charabi, Y., 2018.
845 Potential changes in the number of wet days and its effect on future intense and annual
846 precipitation in northern Oman. *Hydrology Research* 49, 237–250.
847 <https://doi.org/10.2166/nh.2017.188>
- 848 Hamed, K.H., 2008. Trend detection in hydrologic data: The Mann-Kendall trend test under
849 the scaling hypothesis. *J Hydrol (Amst)* 349, 350–363.
850 <https://doi.org/10.1016/j.jhydrol.2007.11.009>
- 851 Hamed, M.M., Ali, Z., Nashwan, M.S., Shahid, S., 2023a. Exposed Population to Hot and Cold
852 Extremes in MENA for Paris Climate Agreement Temperature Goals.
853 <https://doi.org/10.21203/rs.3.rs-2476467/v1>
- 854 Hamed, M.M., Iqbal, Z., Nashwan, M.S., Kineber, A.F., Shahid, S., 2023b. Diminishing
855 evapotranspiration paradox and its cause in the Middle East and North Africa. *Atmos Res*
856 289, 106760. <https://doi.org/10.1016/j.atmosres.2023.106760>
- 857 Hamed, M.M., Nashwan, M.S., Shahid, S., 2021. Performance evaluation of reanalysis
858 precipitation products in Egypt using fuzzy entropy time series similarity analysis.
859 *International Journal of Climatology* 41, 5431–5446. <https://doi.org/10.1002/joc.7286>

- 860 Hamed, M.M., Nashwan, M.S., Shahid, S., Ismail, T. bin, Wang, X., Dewan, A., Asaduzzaman,
861 M., 2022. Inconsistency in historical simulations and future projections of temperature
862 and rainfall: A comparison of CMIP5 and CMIP6 models over Southeast Asia. *Atmos Res*
863 265, 105927. <https://doi.org/10.1016/j.atmosres.2021.105927>
- 864 Hereher, M.E., 2016. Recent trends of temperature and precipitation proxies in Saudi Arabia:
865 implications for climate change. *Arabian Journal of Geosciences* 9.
866 <https://doi.org/10.1007/s12517-016-2605-5>
- 867 Hersbach, H., Bell, B., Berrisford, P., Hirahara, S., Horányi, A., Muñoz-Sabater, J., Nicolas, J.,
868 Peubey, C., Radu, R., Schepers, D., Simmons, A., Soci, C., Abdalla, S., Abellan, X., Balsamo,
869 G., Bechtold, P., Biavati, G., Bidlot, J., Bonavita, M., Chiara, G., Dahlgren, P., Dee, D.,
870 Diamantakis, M., Dragani, R., Flemming, J., Forbes, R., Fuentes, M., Geer, A., Haimberger,
871 L., Healy, S., Hogan, R.J., Hólm, E., Janisková, M., Keeley, S., Laloyaux, P., Lopez, P., Lupu,
872 C., Radnoti, G., Rosnay, P., Rozum, I., Vamborg, F., Villaume, S., Thépaut, J., 2020. The
873 ERA5 global reanalysis. *Quarterly Journal of the Royal Meteorological Society* 146, 1999–
874 2049. <https://doi.org/10.1002/qj.3803>
- 875 Horan, M.F., Batibeniz, F., Kucharski, F., Almazroui, M., Abid, M.A., Fu, J.S., Ashfaq, M., 2023.
876 Moisture sources for precipitation variability over the Arabian Peninsula. *Clim Dyn*.
877 <https://doi.org/10.1007/s00382-023-06762-2>
- 878 Islam, H.M.T., Islam, A.R.M.T., Abdullah-Al-Mahbub, M., Shahid, S., Tasnuva, A.,
879 Kamruzzaman, M., Hu, Z., Elbeltagi, A., Kabir, M.M., Salam, M.A., Ibrahim, S.M., 2021.
880 Spatiotemporal changes and modulations of extreme climatic indices in monsoon-
881 dominated climate region linkage with large-scale atmospheric oscillation. *Atmos Res*
882 264, 105840. <https://doi.org/10.1016/j.atmosres.2021.105840>
- 883 Jiang, L., Zhang, J., Liu, Q., Meng, X., Shi, L., Zhang, D., Xing, M., 2023. Spatiotemporal
884 variations of the global compound heat wave and the drivers of its spatial heterogeneity.
885 *J Clean Prod* 408, 137201. <https://doi.org/10.1016/j.jclepro.2023.137201>
- 886 Jiang, Q., Li, W., Fan, Z., He, X., Sun, W., Chen, S., Wen, J., Gao, J., Wang, J., 2021. Evaluation
887 of the ERA5 reanalysis precipitation dataset over Chinese Mainland. *J Hydrol (Amst)* 595.
888 <https://doi.org/10.1016/j.jhydrol.2020.125660>
- 889 Kaiser-Weiss, A.K., Borsche, M., Niermann, D., Kaspar, F., Lussana, C., Isotta, F.A., van den
890 Besselaar, E., van der Schrier, G., Undén, P., 2019. Added value of regional reanalyses for
891 climatological applications. *Environ Res Commun* 1, 071004.
892 <https://doi.org/10.1088/2515-7620/ab2ec3>
- 893 Kalnay, E., Kanamitsu, M., Kistler, R., Collins, W., Deaven, D., Gandin, L., Iredell, M., Saha, S.,
894 White, G., Woollen, J., Zhu, Y., Leetmaa, A., Reynolds, R., Chelliah, M., Ebisuzaki, W.,
895 Higgins, W., Janowiak, J., Mo, K.C., Ropelewski, C., Wang, J., Jenne, R., Joseph, D., 1996.
896 The NCEP/NCAR 40-Year Reanalysis Project. *Bull Am Meteorol Soc* 77, 437–471.
897 [https://doi.org/10.1175/1520-0477\(1996\)077<0437:TNYRP>2.0.CO;2](https://doi.org/10.1175/1520-0477(1996)077<0437:TNYRP>2.0.CO;2)
- 898 Karl, T.R., Nicholls, N., Ghazi, A., 1999. Clivar/GCOS/WMO Workshop on Indices and Indicators
899 for Climate Extremes Workshop Summary. *Clim Change* 42, 3–7.
900 <https://doi.org/10.1023/A:1005491526870>
- 901 Khadka, D., Babel, M.S., Abatan, A.A., Collins, M., 2022. An evaluation of <sc>CMIP5</sc>
902 and <sc>CMIP6</sc> climate models in simulating summer rainfall in the Southeast

- 903 Asian monsoon domain. *International Journal of Climatology* 42, 1181–1202.
904 <https://doi.org/10.1002/joc.7296>
- 905 Khan, N., Pour, S.H., Shahid, S., Ismail, T., Ahmed, K., Chung, E., Nawaz, N., Wang, X., 2019.
906 Spatial distribution of secular trends in rainfall indices of Peninsular Malaysia in the
907 presence of long-term persistence. *Meteorological Applications* 26, 655–670.
908 <https://doi.org/10.1002/met.1792>
- 909 Komurcu, M., Schlosser, C.A., Alshehri, I., Alshahrani, T., Alhayaza, W., Alsaati, A., Strzepek, K.,
910 2020. Mid-century changes in the mean and extreme climate in the kingdom of Saudi
911 Arabia and implications for water harvesting and climate adaptation. *Atmosphere (Basel)*
912 11. <https://doi.org/10.3390/atmos11101068>
- 913 Kotwicki, V., al Sulaimani, Z., 2009. Climates of the Arabian Peninsula – past, present, future.
914 *Int J Clim Chang Strateg Manag* 1, 297–310.
915 <https://doi.org/10.1108/17568690910977500>
- 916 Kwarteng, A.Y., Dorvlo, A.S., Kumar, G.T.V., 2009. Analysis of a 27-year rainfall data (1977-
917 2003) in the Sultanate of Oman. *International Journal of Climatology* 29, 605–617.
918 <https://doi.org/10.1002/joc.1727>
- 919 Lei, X., Xu, W., Chen, S., Yu, T., Hu, Z., Zhang, M., Jiang, L., Bao, R., Guan, X., Ma, M., Wei, J.,
920 Feng, A., Gao, L., 2022. How Well Does the ERA5 Reanalysis Capture the Extreme Climate
921 Events Over China? Part I: Extreme Precipitation. *Front Environ Sci* 10.
922 <https://doi.org/10.3389/fenvs.2022.921658>
- 923 Li, D., Yuan, J., Kopp, R.E., 2020. Escalating global exposure to compound heat-humidity
924 extremes with warming. *Environmental Research Letters* 15, 064003.
925 <https://doi.org/10.1088/1748-9326/ab7d04>
- 926 Li, H., Liu, G., Han, C., Yang, Y., Chen, R., 2022. Quantifying the Trends and Variations in the
927 Frost-Free Period and the Number of Frost Days across China under Climate Change
928 Using ERA5-Land Reanalysis Dataset. *Remote Sens (Basel)* 14, 2400.
929 <https://doi.org/10.3390/rs14102400>
- 930 Lin, L., Gao, T., Luo, M., Ge, E., Yang, Y., Liu, Z., Zhao, Y., Ning, G., 2020. Contribution of
931 urbanization to the changes in extreme climate events in urban agglomerations across
932 China. *Science of The Total Environment* 744, 140264.
933 <https://doi.org/10.1016/j.scitotenv.2020.140264>
- 934 Ma, H., Zeng, J., Zhang, X., Fu, P., Zheng, D., Wigneron, J.P., Chen, N., Niyogi, D., 2021.
935 Evaluation of six satellite- and model-based surface soil temperature datasets using
936 global ground-based observations. *Remote Sens Environ* 264, 112605.
937 <https://doi.org/10.1016/j.rse.2021.112605>
- 938 Mansour, S., 2019. Geospatial modelling of tropical cyclone risks to the southern Oman coasts.
939 *International Journal of Disaster Risk Reduction* 40, 101151.
940 <https://doi.org/10.1016/j.ijdrr.2019.101151>
- 941 Mavromatis, T., 2022. Evaluation of Reanalysis Data in Meteorological and Climatological
942 Applications: Spatial and Temporal Considerations. *Water (Basel)* 14, 2769.
943 <https://doi.org/10.3390/w14172769>

- 944 Nakamura, H., Kuma, K., Onogi, K., Miyasaka, T., Makihara, Y., Ishida, J., Iida, M., 2022. Toward
945 High-Resolution Regional Atmospheric Reanalysis for Japan: An Overview of the
946 ClimCORE Project, in: 2022 IEEE International Conference on Big Data (Big Data). IEEE,
947 pp. 6153–6158. <https://doi.org/10.1109/BigData55660.2022.10020656>
- 948 Nashwan, M.S., Shahid, S., Abd Rahim, N., 2019. Unidirectional trends in annual and seasonal
949 climate and extremes in Egypt. *Theor Appl Climatol* 136, 457–473.
950 <https://doi.org/10.1007/s00704-018-2498-1>
- 951 Nasrallah, H.A., Balling, R.C., 1996. Analysis of recent climatic changes in the Arabian Peninsula
952 region. *Theor Appl Climatol* 53, 245–252. <https://doi.org/10.1007/BF00871740>
- 953 Ng, C.Y., Wan Jaafar, W.Z., Mei, Y., Othman, F., Lai, S.H., Liew, J., 2022. Assessing the Changes
954 of Precipitation Extremes in Peninsular Malaysia. *International Journal of Climatology*.
955 <https://doi.org/10.1002/joc.7684>
- 956 Odnoletkova, N., Patzek, T.W., 2021. Data-driven analysis of climate change in Saudi Arabia:
957 trends in temperature extremes and human comfort indicators. *J Appl Meteorol
958 Climatol*. <https://doi.org/10.1175/JAMC-D-20-0273.1>
- 959 Patakamuri, S.K., O'Brien, N., 2021. modifiedmk: Modified Versions of Mann Kendall and
960 Spearman's Rho Trend Tests [WWW Document]. R package version 1.6. URL
961 <https://CRAN.R-project.org/package=modifiedmk> (accessed 7.23.23).
- 962 Peaklist.org, 2006. Arabian Peninsula and Middle East [WWW Document]. URL
963 <http://www.peaklist.org/WWlists/ultras/mideast.html#Footnotes> (accessed 9.8.19).
- 964 Pohlert, T., 2023. trend: Non-Parametric Trend Tests and Change-Point Detection [WWW
965 Document]. R package version 1.1.5. URL <https://CRAN.R-project.org/package=trend>
966 (accessed 7.23.23).
- 967 QGIS Development Team, 2023. QGIS Geographic Information System [WWW Document].
968 URL <https://www.qgis.org/en/site/> (accessed 7.23.23).
- 969 R Core Team, 2023. R: A Language and Environment for Statistical Computing. R Foundation
970 for Statistical Computing.
- 971 Randriatsara, H.H.R.H., Hu, Z., Xu, X., Ayugi, B., Sian, K.T.C.L.K., Mumo, R., Ongoma, V., 2022.
972 Evaluation of gridded precipitation datasets over Madagascar. *International Journal of
973 Climatology* 42, 7028–7046. <https://doi.org/10.1002/joc.7628>
- 974 Rashid, I.U., Almazroui, M., Saeed, S., Atif, R.M., 2020. Analysis of extreme summer
975 temperatures in Saudi Arabia and the association with large-scale atmospheric
976 circulation. *Atmos Res* 231. <https://doi.org/10.1016/j.atmosres.2019.104659>
- 977 Sa'adi, Z., Yaseen, Z.M., Farooque, A.A., Mohamad, N.A., Muhammad, M.K.I., Iqbal, Z., 2023.
978 Long-term trend analysis of extreme climate in Sarawak tropical peatland under the
979 influence of climate change. *Weather Clim Extrem* 40, 100554.
980 <https://doi.org/10.1016/j.wace.2023.100554>
- 981 Saeed, S., Kucharski, F., Almazroui, M., 2023. Impacts of mid-latitude circulation on winter
982 temperature variability in the Arabian Peninsula: the explicit role of NAO. *Clim Dyn* 60,
983 147–164. <https://doi.org/10.1007/s00382-022-06313-1>

- 984 Safieddine, S., Clerbaux, C., Clarisse, L., Whitburn, S., Eltahir, E.A.B., 2022. Present and future
985 land surface and wet bulb temperatures in the Arabian Peninsula. *Environmental*
986 *Research Letters* 17. <https://doi.org/10.1088/1748-9326/ac507c>
- 987 Saleh M. Billo, 1982. Petroleum Geology of Arabian Peninsula: ABSTRACT. *Am Assoc Pet Geol*
988 *Bull* 66. <https://doi.org/10.1306/03B59BE3-16D1-11D7-8645000102C1865D>
- 989 Schulman, S., 2021. Yemenis' Daily Struggles Between Conflict and Climate Change. *The RUSI*
990 *Journal* 166, 82–92. <https://doi.org/10.1080/03071847.2021.1922196>
- 991 Sedaoui, R., 2022. Energy and the Economy in the Middle East and North Africa, in: *The*
992 *Palgrave Handbook of International Energy Economics*. Springer International
993 Publishing, Cham, pp. 667–691. https://doi.org/10.1007/978-3-030-86884-0_33
- 994 Sen, P.K., 1968. Estimates of the Regression Coefficient Based on Kendall's Tau. *J Am Stat*
995 *Assoc* 63, 1379–1389. <https://doi.org/10.1080/01621459.1968.10480934>
- 996 Shahid, S., 2010. Rainfall variability and the trends of wet and dry periods in Bangladesh.
997 *International Journal of Climatology* 30, 2299–2313. <https://doi.org/10.1002/joc.2053>
- 998 Sun, X., Ren, G., You, Q., Ren, Y., Xu, W., Xue, X., Zhan, Y., Zhang, S., Zhang, P., 2019. Global
999 diurnal temperature range (DTR) changes since 1901. *Clim Dyn* 52, 3343–3356.
1000 <https://doi.org/10.1007/s00382-018-4329-6>
- 1001 Tarawneh, Q.Y., Chowdhury, S., 2018. Trends of climate change in Saudi Arabia: Implications
1002 on water resources. *Climate* 6. <https://doi.org/10.3390/cli6010008>
- 1003 Velikou, K., Lazoglou, G., Tolika, K., Anagnostopoulou, C., 2022. Reliability of the ERA5 in
1004 Replicating Mean and Extreme Temperatures across Europe. *Water (Basel)* 14, 543.
1005 <https://doi.org/10.3390/w14040543>
- 1006 Walt, A.J., Fitchett, J.M., 2021. Trend analysis of cold extremes in South Africa: 1960–2016.
1007 *International Journal of Climatology* 41, 2060–2081. <https://doi.org/10.1002/joc.6947>
- 1008 WHO, 2018. Health and climate change [WWW Document]. [https://www.who.int/news-](https://www.who.int/news-room/facts-in-pictures/detail/health-and-climate-change)
1009 [room/facts-in-pictures/detail/health-and-climate-change](https://www.who.int/news-room/facts-in-pictures/detail/health-and-climate-change).
- 1010 WMO, 2021. Guide to Instruments and Methods of Observation Volume I-Measurement of
1011 Meteorological Variables [WWW Document]. URL
1012 https://library.wmo.int/index.php?id=12407&lvl=notice_display (accessed 7.4.23).
- 1013 Xu, W., Lei, X., Chen, S., Yu, T., Hu, Z., Zhang, M., Jiang, L., Bao, R., Guan, X., Ma, M., Wei, J.,
1014 Gao, L., Feng, A., 2022. How Well Does the ERA5 Reanalysis Capture the Extreme Climate
1015 Events Over China? Part II: Extreme Temperature. *Front Environ Sci* 10.
1016 <https://doi.org/10.3389/fenvs.2022.921659>
- 1017 You, Q., Fraedrich, K., Min, J., Kang, S., Zhu, X., Ren, G., Meng, X., 2013. Can temperature
1018 extremes in China be calculated from reanalysis? *Glob Planet Change* 111, 268–279.
1019 <https://doi.org/10.1016/j.gloplacha.2013.10.003>
- 1020 Yue, S., Wang, C., 2004. The Mann-Kendall Test Modified by Effective Sample Size to Detect
1021 Trend in Serially Correlated Hydrological Series. *Water Resources Management* 18, 201–
1022 218. <https://doi.org/10.1023/B:WARM.0000043140.61082.60>
- 1023 Zhang, X., Aguilar, E., Sensoy, S., Melkonyan, H., Tagiyeva, U., Ahmed, N., Kutladze, N.,
1024 Rahimzadeh, F., Taghipour, A., Hantosh, T.H., Albert, P., Semawi, M., Karam Ali, M., Said

- 1025 Al-Shabibi, M.H., Al-Oulan, Z., Zadari, T., Al Dean Khelet, I., Hamoud, S., Sagir, R.,
1026 Demircan, M., Eken, M., Adiguzel, M., Alexander, L., Peterson, T.C., Wallis, T., 2005.
1027 Trends in Middle East climate extreme indices from 1950 to 2003. *J Geophys Res* 110,
1028 D22104. <https://doi.org/10.1029/2005JD006181>
- 1029 Zhao, N., Jiao, Y., Ma, T., Zhao, M., Fan, Z., Yin, X., Liu, Y., Yue, T., 2019. Estimating the effect
1030 of urbanization on extreme climate events in the Beijing-Tianjin-Hebei region, China.
1031 *Science of The Total Environment* 688, 1005–1015.
1032 <https://doi.org/10.1016/j.scitotenv.2019.06.374>
- 1033 Zhao, P., He, Z., Ma, D., Wang, W., 2023. Evaluation of ERA5-Land reanalysis datasets for
1034 extreme temperatures in the Qilian Mountains of China. *Front Ecol Evol* 11.
1035 <https://doi.org/10.3389/fevo.2023.1135895>
- 1036 Zittis, G., Almazroui, M., Alpert, P., Ciais, P., Cramer, W., Dahdal, Y., Fnais, M., Francis, D.,
1037 Hadjinicolaou, P., Howari, F., Jrrar, A., Kaskaoutis, D.G., Kulmala, M., Lazoglou, G.,
1038 Mihalopoulos, N., Lin, X., Rudich, Y., Sciare, J., Stenchikov, G., Xoplaki, E., Lelieveld, J.,
1039 2022. Climate Change and Weather Extremes in the Eastern Mediterranean and Middle
1040 East. *Reviews of Geophysics* 60. <https://doi.org/10.1029/2021RG000762>
- 1041 Zuluaga, C.F., Avila-Diaz, A., Justino, F.B., Wilson, A.B., 2021. Climatology and trends of
1042 downward shortwave radiation over Brazil. *Atmos Res* 250, 105347.
1043 <https://doi.org/10.1016/j.atmosres.2020.105347>
- 1044